JPhys Materials

PAPER • OPEN ACCESS

Interactions of different hydrocolloids with milk proteins

IOP Publishing J. Phys. Mater. 3 (2020) 044003 https://doi.org/10.1088/2515-7639/aba2b7

Journal of Physics: Materials

OPEN ACCESS

RECEIVED
14 April 2020

REVISED
15 June 2020

ACCEPTED FOR PUBLICATION
3 July 2020

PUBLISHED
20 August 2020

PAPER

Interactions of different hydrocolloids with milk proteins

Judith Hege[1], **Thomas Palberg**[2] **and Thomas A Vilgis**[1]

[1] Max Planck Institute for Polymer Research, Ackermannweg 10, 55128 Mainz, Germany
[2] Johannes Gutenberg University, Institute of Physics, Staudingerweg 7, 55099 Mainz, Germany

E-mail: hege01@mpip-mainz.mpg.de **and** vilgis@mpip-mainz.mpg.de

Keywords: whey proteins, casein micelles, xanthan gum, guar gum, iota-carrageenan, gellan gum, hydrocolloids

Abstract

To control rheological properties and accomplish perfect sensory properties and mouthfeel, polysaccharides are added to milk-based beverages. However, in contrast to expectations, it is often found that adding low concentrations of xanthan gum or guar gum to milk provokes phase separations of unclear physical origin. From this observation, questions arise regarding the interaction of added polysaccharides and the proteins present in milk – caseins and whey proteins. The focus of this study is to investigate such systems and to understand the basic interactions of caseins and whey proteins with different hydrocolloids. The hydrocolloids used in this study are xanthan gum, guar gum, gellan gum as well as iota-carrageenan, which were dissolved in pasteurized, non-homogenized, skimmed milk. The methods used for the examinations are light microscopy, measurement of zeta potential, atomic force microscopy and measurement of particle sizes. It was found for the case of xanthan gum dissolved in milk that the xanthan gum molecules and some of the whey proteins are found in the upper phase whereas the casein micelles as well as whey proteins are in the lower phase. For the case of guar gum dissolved in milk, the guar gum molecules are present in the upper phase and the casein micelles are present in the lower phase. This phase separation is probably caused by depletion interaction. Whey proteins are found in both phases. For the cases of iota-carrageenan, respectively, gellan gum dissolved in milk no macroscopic phase separation is observed and the measurements suggest the formation of complexes between the hydrocolloid and whey proteins.

1. Introduction

Bovine milk is a common food in most cultures [1] which has been used for human nutrition since time immemorial. In sports nutrition particularly, whey proteins and caseins - the proteins present in milk – are of great interest to body builders since they are a very important source of protein to build up muscles [2]. On the other hand, it is often difficult to control viscosity and flow behaviour of such drinks by natural milk proteins in a well controlled way.

There exists a wide variety of food grade polar polymers and polyelectrolytes (so called hydrocolloids) that are used to regulate the flow properties and the texture of fluids [3]. These carbohydrate and carbohydrate derived molecules can be used to thicken or gel liquid foods but also to stabilize drinks that are mixed of different components [4]. In such drinks only low concentrations of about 0.01–0.025 wt% of the chosen hydrocolloid are used. These concentrations far below the overlap concentration c^* [5] are sufficiently high to stabilize the system but maintain the viscosity low enough to ensure a pleasant texture and drinkability.

However, these simple attempts define a number of non-trivial problems, since milk is a complex system consisting of numerous components and the addition of hydrocolloids impacts the entropy of the system and changes the free energy of the system. The interactions between the different milk components and the added hydrocolloid particles have to be considered in order to understand the system and its microscopic as well as macroscopic behaviour.

Milk contains about 3.3% of protein as well as about 4.7% of lactose [6], salts and vitamins that are dissolved in water. There are two fractions of proteins: 2.7% casein as well as 0.6% whey protein [1].

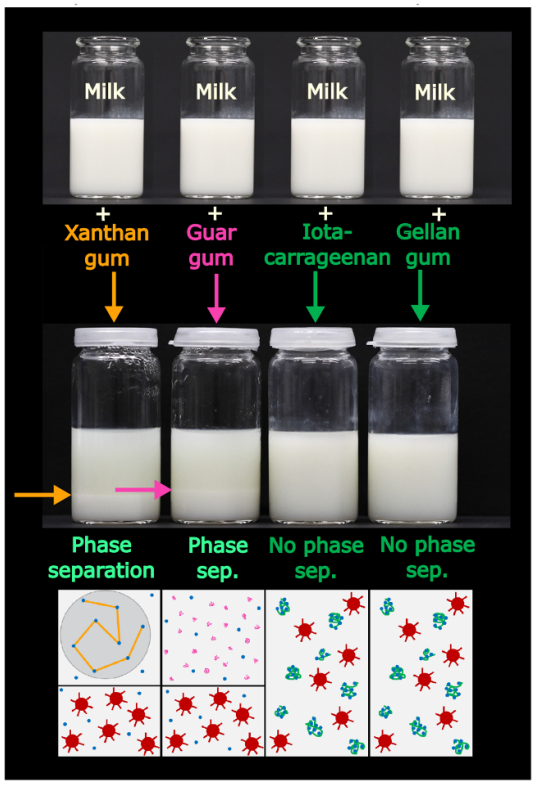

Graphical abstract

The four types of caseins, α_{S1}-, α_{S2}-, β- and κ-casein [7], form micelles in an aqueous environment, since only κ-casein contains a hydrophilic part [8]. A simplified model of a casein micelle is shown in figure 1. The α_{S1}-, α_{S2}- and β-caseins in the inner part of the micelles build hydrophobic submicelles (marked in red in figure 1) which are connected to each other via calcium phosphate bridging bonds (black dots in figure 1). The κ-caseins are situated on the outside of submicelles to form the overall micelle surface. Their hydrophilic parts (blue arms in figure 1) ensure the solubility in the whey [9]. The hydrophilic parts of the κ-caseins have an overall weak negative net charge in native milk, where the pH-value is about 6.6 to 6.8 [6]. Therefore two mechanisms contribute to the casein stability: the steric hindrance by the κ-casein 'arms' and the overall negative net charge of the micelles at their surface. Casein micelles are thus highly stable even when milk is heated. The volume-average radius of a casein micelle is about 61 nm [9].

The whey proteins of importance are β-lactoglobulin which makes 56% of the whey protein fraction and α-lactalbumin with 21%. Furthermore, there are immunoglobulins providing 14% of the whey proteins, serum albumin with 8% and lactoferrin with 2% [6]. In milk,whey proteins exist in their globular form and remain dissolved due to their surface charges. Figure 2 shows models of the dominant whey proteins.

Different salts and ions are present in milk. Only the minority is directly dissolved in the whey, others form complexes and the majority is bound in colloidal complexes (casein micelles) or at macromolecules. Calcium is present with a concentration of $1.0-1.4\ \mathrm{g l^{-1}}$ (about 30 mM). Roughly one third of it can be found in the watery phase (whey). Only 2 to 3 mM from that are free Ca^{2+} ions. The other 7 to 8 mM form complexes with phosphate and citrate and are bound inside the casein submicelles. The main part, about 20 mM, are bound together with the phosphates in the casein micelles by balancing charges between proteins [6].

It has been shown previously that adding xanthan gum to pure milk induces phase separations under certain conditions [15, 16]. Also, if guar gum is added to milk a phase separation is provoked even though these molecules have a quite different chemical structure [17, 18]. Other hydrocolloids like gellan gum [19] and iota-carrageenan [20, 21] do not show a macroscopic phase separation. The present study focuses on the physical interactions in such systems at the molecular level in order to explain the phenomenon of those phase separations. To pursue this goal, four different hydrocolloids with very different chemical structure were chosen and compared to each other, namely xanthan gum, guar gum, iota-carrageenan as well as gellan gum. Chemical structures are shown in figure 3. The four hydrocolloids used in this study are polysaccharides commonly used by the food industry in varius applications [22, 23]. However, they show a

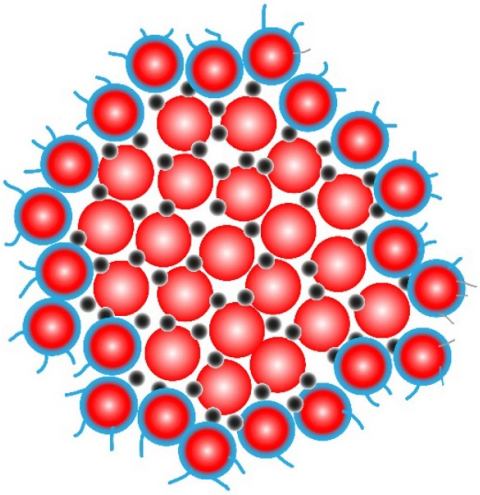

Figure 1. Schematic representation of the casein micelle structure. α_{S1}-, α_{S2}- and β-caseins form hydrophobic submicelles (red spheres) that are located in the inner part of a casein micelle and are connected via calcium phosphate bridging bonds (black dots). The κ-caseins at the surface (blue) ensure the solubility in the whey. Reproduced from [10].

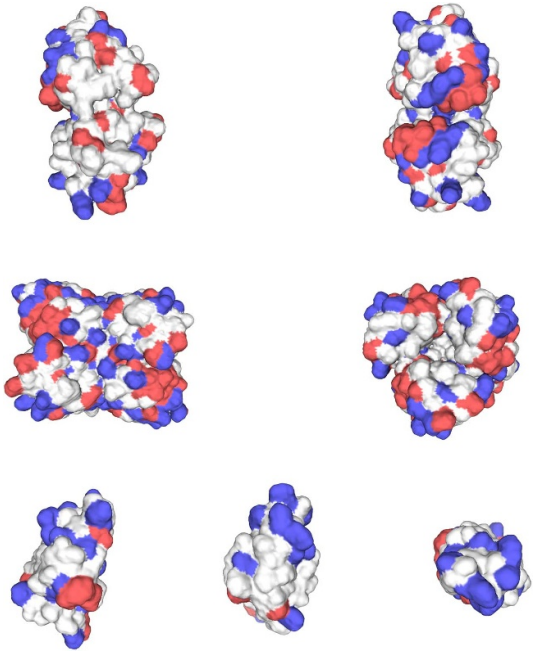

Figure 2. Surface of globular whey proteins from different perspectives. Upper row: β-Lactoglobulin dimer. Source: [11, 12]. Middle row: α-lactalbumin. Source: [12, 13]. Lower row: serum albumin. Source: [12, 14]. Positively charged (basic) amino acids are coloured blue, negatively charged (acidic) ones are red.

different behaviour when added to milk. Xanthan gum and guar gum provoke a phase separation in milk whereas iota-carrageenan and gellan gum do not. Guar gum is an uncharged molecule whereas xanthan gum, iota-carrageenan as well as gellan gum are negatively charged molecules. The chosen polysaccharides also vary in flexibility/ stiffness of the molecule.

These remarks show already, that the molecular structure and the charges of added hydrocolloids matter. The interplay between sizes of casein micelles and neutral flexible hydrocolloid (guar gum), electrostatic interactions between amphiphilic whey proteins, negative charged hydrocolloids of different chain flexibility will determine the phase behaviour of the colloidal fluids. Even small concentrations far below the overlap concentration c^* of the hydrocolloids will induce macroscopic effects. Therefore is shown below, that depletion interactions [24] are the main driving force for the phase separation.

The main intention is drawn on the interaction between each of the four hydrocolloids, respectively, with the milk proteins (whey proteins as well as casein micelles). For this reason the milk was skimmed via

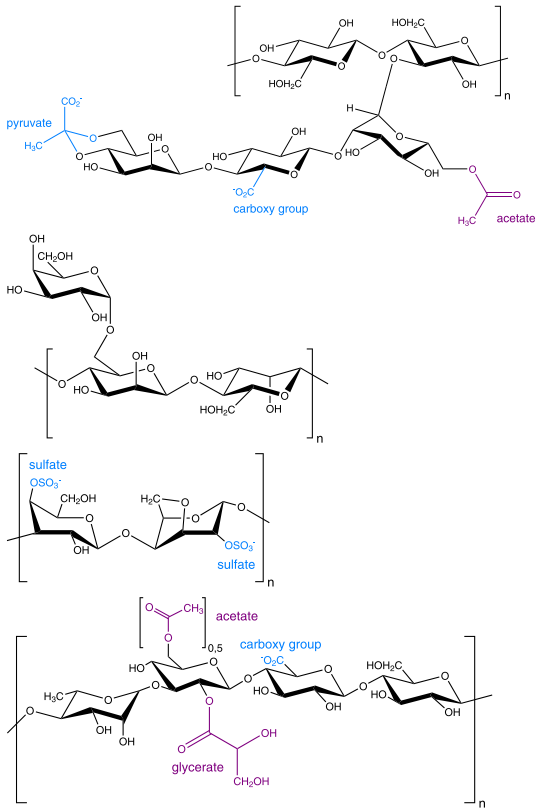

Figure 3. Chemical structure of the hydrocolloids. From top to bottom: xanthan gum, guar gum, iota-carrageenan and high-acyl gellan gum. Source: own representation.

centrifugation to remove fat. Still, skimmed milk remains a very complex system with many different components [25], which may have impact on the interactions. To minimise such side effects, milk standards need to be prepared, as described further below.

The main experimental methods that are used in this study are optical microscopy, atomic force microscopy [26], measurement of zeta potential [27] and measurement of particle size distribution [28] to gain further understanding in the molecular interplay between the different milk proteins and hydrocolloids.

To place this study in the broader topic of milk additives it has to be mentioned that the addition of salts to milk affects the natural salt and ion balance in the milk as well as the stability of the casein micelles [29]. Furthermore, different kinds of flavours can be added to milk. The effects of tea, coffee, and cocoa extracts on milk under heating were for example studied by O'Connell *et al* [30], especially in cases where additives sediment the hydrocolloids come into play to stabilize the system. For this reason, the current study plays an important role, since it shows that not every polysaccharide can be used for this purpose. In order to improve the stabilising function of e.g. xanthan gum, it can be thought of manipulating the properties of this molecule by making it more flexible or screening its surface charges by adding for example twice positively charged calcium ions.

2. Materials and methods

2.1. Investigated systems

To study the interactions of milk proteins with xanthan gum, guar gum, iota-carrageenan and gellan gum, respectively, *Heumilch* from the local store and always the same producer (*Gläserne Molkerei*) was chosen as matrix. This milk is non-homogenized, but pasteurized (i.e. heated to 72 °C for 15 s [6]). Since the milk was not homogenized the fat is still in its natural composition and size distribution and is resulting in creaming after some time. The fat content of the milk is 3.8% fat (as per packaging). For each experiment in the present study the milk was skimmed by centrifuging it for 20 min at a speed of 6414× g at 4 °C (according to the study of R Trejo *et al* [31]) using a Thermo Scientific Multifuge X1R (Thermo Fisher Scientific, 168 Third Avenue, Waltham, MA USA 02 451). At this temperature the milk fat is still mainly solid so it can easily be taken off with a spoon. Furthermore, rapid bacterial growth is prevented by choosing a low temperature as maximum bacterial growth in foods has been reported between 20 °C and 30 °C [32, 33] and minimum growth at −10 °C [33, 34].

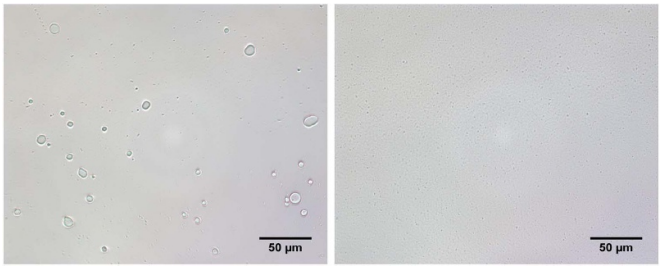

Figure 4. Microscopy pictures of skimmed milk. Magnification 400 ×. Left: creamed fat taken off with a spoon. There are still some fat droplets. Right: after filtering with a 0.8 μm syringe filter.

Immediately after centrifuging, the creaming layer was removed from the milk using a spoon. The remaining fat droplets were filtered by using syringe filters with pore sizes of 5 μm, 1.2 μm and 0.8 μm. This way virtually all fat should be removed from the milk while at the same time the casein micelles (130 nm diameter) should still be in their native composition and shape which was considered to be crucial in this study. Figure 4 shows microscopy pictures of the skimmed milk.

Heumilch from *Gläserne Molkerei* was chosen because it is produced from a limited number of farms and cows. The milk is collected from about 130 organic farmers who each hosts between 10 to 500 cows. All cows are on pasture during summer time and are fed hay during the winter period. No silage is used which would have caused stronger deviations in the milk composition [35]. The protein content according to the packaging is 3.4 g in 100 ml.

The following gum types were used: xanthan gum from Jungbunzlauer (JUNGBUNZLAUER SUISSE AG, St. Alban-Vorstadt 90, CH-4002 Basel, Switzerland), guar gum from Unipektin (UNIPEKTIN Ingredients AG, Bahnhofstrasse 9, CH-8264 Eschenz, Switzerland), ultrapure iota-carrageenan from Carl Roth (Carl Roth GmbH + Co. KG, Schoemperlenstr. 1−5, 76 185 Karlsruhe) and food-grade high acyl gellan gum from CP Kelco (CP Kelco U.S., Inc. Cumberland Center II, 3100 Cumberland Boulevard, Suite 600, Atlanta, GA 30 339, USA). They are all white or off-white powders that were dissolved in milliQ water (18.2 MΩ·cm) and milk, respectively. The hydrocolloid concentration for all samples was 0.1 wt%, where the mixtures remain liquid. This feature was important for the industrial application of stabilizing milk-based beverages. All samples containing milk were kept at 4 °C.

Xanthan gum and guar gum were dissolved by stirring at 600 rpm for 18 h at room temperature (milliQ water: 18.2 MΩ·cm) or in the fridge at 4 °C (milk). Iota-carrageenan was heated under stirring at 600 rpm to 70 °C and kept at this temperature for 20 min, whereas gellan gum was heated to 80 °C and kept there for 20 min.

The whey protein isolate (sure protein WPI 895) used for some of the experiments came from the company nzmp (nzmp is a brand of Fonterra Co-operative Group, 109 Fanshawe Street, Auckland 1020, New Zealand). Whey protein isolate is produced from fresh cheese whey by microfiltration or ion exchange. Afterwards it is ultrafiltrated and then evaporated and spray-dried [36].

2.2. Light microscope

With the optical microscope Axio Scope.A1 from Carl Zeiss (Carl Zeiss AG, Carl-Zeiss-Straße 22, 73 447 Oberkochen, Germany) pictures of milk samples were taken in transmission bright field microscopy at magnifications of 100 ×, 200 ×, 400 × and 1000 ×. Photos were taken of milk with fat and after each step of skimming as well as of milk mixed with each of the hydrocolloids, respectively. In case of phase separation photos were taken of the upper as well as of the lower phase. A droplet of the sample was taken with a pipette and was put onto a microscope slide. The droplet was then covered with a cover slip. Besides that, another preparation method was used as well - droplet evaporation. The droplet was put onto the microscope slide and then put into a box to prevent any disturbance by air flow. The small droplet (2 μl) dried over night and was viewed with the optical microscope after 24 hours without a cover slip.

2.3. Zetasizer

Zeta potential was measured for whey protein dissolved in milliQ water, whey protein and hydrocolloid dissolved in milliQ water, skimmed not homogenized milk (*Heumilch*), as well as hydrocolloids dissolved in skimmed *Heumilch*.

Zeta potential measurements were taken using a Malvern Zetasizer Nano-Z (Malvern Panalytical GmbH, Kassel, Germany). In order to make single particles of the solution detectable for the laser, samples were diluted with milliQ water. The sample concentration in the final solution was 0.001 wt%. All measurements

Figure 5. Macroscopic behaviour of the four different hydrocolloids dissolved in milk (0.1 wt% hydrocolloid). From left to right: xanthan gum, guar gum, iota-carrageenan and gellan gum. Xanthan gum and guar gum show a phase separation whereas iota-carrageenan and gellan gum do not.

were performed at 25 °C and an equilibration time of 120 seconds. For each sample type three identically prepared samples were measured. For each of those samples the cuvette was filled three times and for each cuvette filling three measurements were performed. So in the end there were nine measurements for each sample and thus 27 measurements of each sample type. The Malvern Zetasizer Nano-Z gives a zeta potential value as well as a value for the standard deviation for each measurement. From those measurement data mean values were calculated.

All milk based samples provided reproducible results. The xanthan gum, as well as gellan gum, dissolved in milliQ water provided reliable results. Guar gum dissolved in milliQ water could not be measured since it is not charged. For iota-carrageenan there was a wider scattering of the measured values than for the other samples. Therefore, no mean value for iota-carrageenan could be given. For samples showing phase separation (xanthan gum in milk and guar gum in milk) each of the phases was measured after 6 h at rest. After this time a clear phase separation had occurred.

2.4. Atomic force microscope

Atomic force microscopy was performed using a MultiMode TUNA TR (Originally: Nanoscope, then: Veeco, today: Bruker Corporation, 40 Manning Road, Billerica, MA 01 821, USA). The cantilevers used had a resonance frequency of 300 kHz and a spring constant of 26 N m^{-1}. All measurements were performed in tapping mode. Samples were prepared as described in section 2.1 'Investigated systems' and then diluted to 10 μg g^{-1}, 1 μg g^{-1} and 0.1 μg g^{-1}. As sample holder a steal plate covered with a mica plate was used. One droplet of 2 μl sample solution was put onto a clean mica surface and then either dried with argon or droplet evaporation underneath a glass cover. For the argon dried samples the droplet was put at the clean mica surface and then allowed to rest for 30 s, so that the particles of the sample could attach to the surface. Then the droplet was dried at the mica plate using an argon stream. For the other samples (droplet evaporation) the droplet was put onto the mica surface, covered by a little petri dish and allowed to dry for about 1 h. For the hydrocolloids dissolved in milliQ water both methods were carried out and the samples investigated using AFM. For pure milk and samples of hydrocolloids dissolved in milk only droplet evaporation was done for all samples, because otherwise the big spheres were not seen. It seemed like at drying with argon the big spheres (probably casein micelles) did not attach strong enough to the mica surface and were blown away from the argon stream. So droplet evaporation would give the 'better', more realistic picture in this case. For every sample pictures were taken at different scan sizes. Usually it was started with an overview of 5 μm and then zoomed in by reducing the scan size. Several pictures were taken for every sample. For each sample at least two different spots were investigated. And also each sample was prepared at least two times to make sure the investigated spot was not an exception. When reducing the scan size usually also the frequency was reduced in order to get sharper structures at the resulting image. Frequencies used were in the range of 1 Hz to 0.3 Hz. To get the final pictures from the raw data the open source software Gwyddion was used which is a data analysis software for scanning probe microscopy (SPM) [37].

2.5. Particle size analyser

Particle size was measured using a Beckman Coulter (Beckman Coulter, Inc. 250 South Kraemer Boulevard, Brea, California 92 821-6232, USA) LS 13 320 Laser Diffraction Particle Size Analyzer for skimmed *Heumilch*, each of the hydrocolloids dissolved in milliQ water and each of the hydrocolloids dissolved in skimmed *Heumilch*.

Guar gum dissolved in milliQ water was centrifuged in order to get rid of cell components that are still present in the guar gum powder. Centrifugation was performed at a speed of 15 000× g at 20 °C for 20 min using a Thermo Scientific Multifuge X1R. As a reference also non-centrifuged guar gum dissolved in milliQ water was measured. Dilution of the samples was done by the particle size analyser. Drops of sample solution were trickled into the measuring cell filled with distilled water until a certain saturation was reached. For the milk and hydrocolloid in milk samples an obscuration of 9−10% was selected (as suggested by Beckman Coulter). The pure hydrocolloid samples were not turbid enough to reach such an obscuration. In this case measurements were performed with an obscuration of 0% which was fine for xanthan gum and gellan gum as well as non-centrifuged guar gum in milliQ water. Only iota-carrageenan and centrifuged guar gum were too clear to give reproducible results.

Every measurement done by the particle size analyser was a three-fold determination. For each sample type three of those three-fold determination measurements were performed. Shown graphs are mean values.

The Beckman Coulter LS 13 320 Laser Diffraction Particle Size Analyzer uses two different sources of illumination. The main light source is a 5 mW laser diode which emits monochromatic light with a wavelength of 780 nm. Additionally, there is a tungsten-halogen lamp which is used in the patented Polarization Intensity Differential Scattering (PIDS) technology. This technology uses the polarization effect of small particles ($d \ll \lambda$, with d the dimension of the particle and λ the wavelength of the incident beam) and combines it with the wavelength dependence of large scattering angles. Thus, the sensitivity of measuring small particle sizes is enhanced and the lower size limit is extended to particle sizes of 40 nm. By projecting the light of the tungsten-halogen lamp through a set of filters three different wavelengths are obtained: 450 nm, 600 nm and 900 nm. Afterwards, the light of each wavelength is polarised using two orthogonally oriented polarisers. The intensity of the scattered light in dependence of the scattering angle (scattering pattern) is measured using 126 detectors. The detectors are placed at different angles from the optical axis. The maximum scattering angle measured is approximately 35°. From the measured scattering pattern the size distribution of the particles in the sample is computed. Furthermore, there are 116 size channels from 0.04 μm to 2000 μm which are spaced logarithmically [38]. The optical model that was used by the particle size analyser is Fraunhofer.rf780d. PIDS (Polarization Intensity Differential Scattering technology) data was included. The Beckman Coulter LS 13 320 Laser Diffraction Particle Size Analyzer brings its own software. Using this software the analysis was performed using Fraunhofer scattering theory. The shown graphs were plotted from the received data using OriginPro 2017 software (OriginLab Corporation, One Roundhouse Plaza, Suite 303, Northampton, MA 01 060, USA).

3. Results

3.1. Macroscopic observation

The hydrocolloids were dissolved in skimmed *Heumilch* as described in Chapter 2 'Materials and methods'. Subsequently, the macroscopic behaviour of the four systems was observed. The samples containing guar gum or xanthan gum began exhibiting a phase separation already after half an hour. After five hours a clear phase separation could be observed. Further observation of the samples revealed that the height of the lower phase remains unchanged over time. For iota-carrageenan and gellan gum no phase separation could be observed, even after a few days. Figure 5 shows the macroscopic behaviour of the four different hydrocolloids dissolved in milk.

All samples look opaque and white. For the phase separated samples the upper phase looks optically slightly thinner than the lower phase and less white. Both phases are liquid. The non-phase separated systems look essentially like pure milk. These samples remain liquid when cooled down slowly and under stirring. Rapid cooling without stirring, on the other hand, results in the formation of a very weak gel.

3.2. Molar mass

Table 1 shows molar masses measured using gel permeation chromatography multi angle light scattering (GPC-MALLS). Displayed are mean values for xanthan gum, guar gum and iota-carrageenan, respectively. For gellan gum the measurement was very difficult and the result had little informative value.

3.3. Light microscope

With optical microscopy undiluted samples can be viewed. Figure 6 shows microscope images of upper and lower phase of xanthan gum dissolved in skimmed *Heumilch*. Surprisingly, there were relatively large spheres appearing in the lower phase. The diameter of selected spheres was measured using ImageJ software [39]. The diameter of these spheres ranges from about 2.4 μm to 15.7 μm, in other pictures also up to 28.9 μm. These spheres have not been observable in pure milk reference samples. Some constituent of the milk-xanthan gum solution appear to be forced (and sedimented) into the lower phase where large

Table 1. Molar masses of xanthan gum, guar gum and iota-carrageenan.

	Xanthan [g mol^{-1}]	Guar [g mol^{-1}]	Iota-carrageenan [g mol^{-1}]
	1206 000	1406 000	381 000
	1632 000	1580 000	248 000
	1418 000	1852 000	308 000
	1730 000		266 000
mean	1496 500	1612 667	300 750

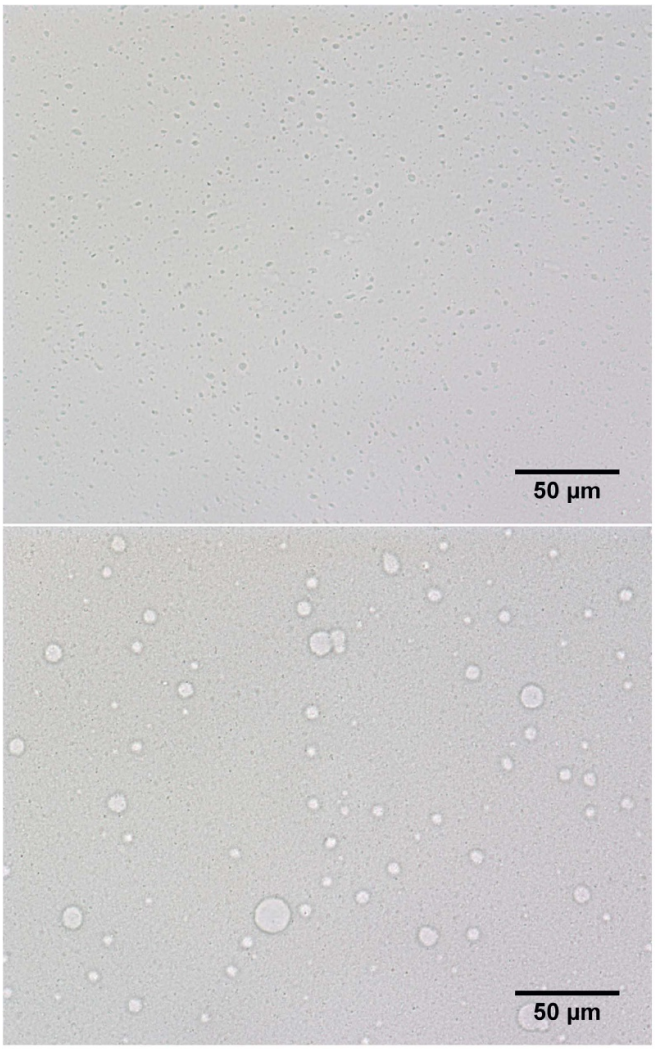

Figure 6. Microscope images of upper (top) and lower (bottom) phase of xanthan gum in milk. Both pictures taken with bright field light microscopy and a magnification of 400×.

agglomerates were formed. As will be seen later from other measurements, xanthan gum was found dominantly in the upper phase. These spheres were most likely formed by several of the casein micelles that were displaced by the xanthan gum molecules.

There was a phase separation observed as well for guar gum dissolved in milk, but in this case no spheres of comparable size could be found in the lower phase. Still, there was slightly more structure in the lower phase to be discovered than in the upper phase. Microscope images of upper and lower phase of guar gum dissolved in skimmed *Heumilch* are shown in figure 7.

For gellan gum and iota-carrageenan no macroscopic phase separation could be observed. But studying the samples by optical microscopy revealed some interesting structures. Even though the samples were liquid under the light microscope it almost seemed as if there was a weak gel that was breaking, especially for the gellan gum sample. Figures 8 and 9 display microscope images of gellan gum dissolved in milk and iota-carrageenan dissolved in milk, respectively.

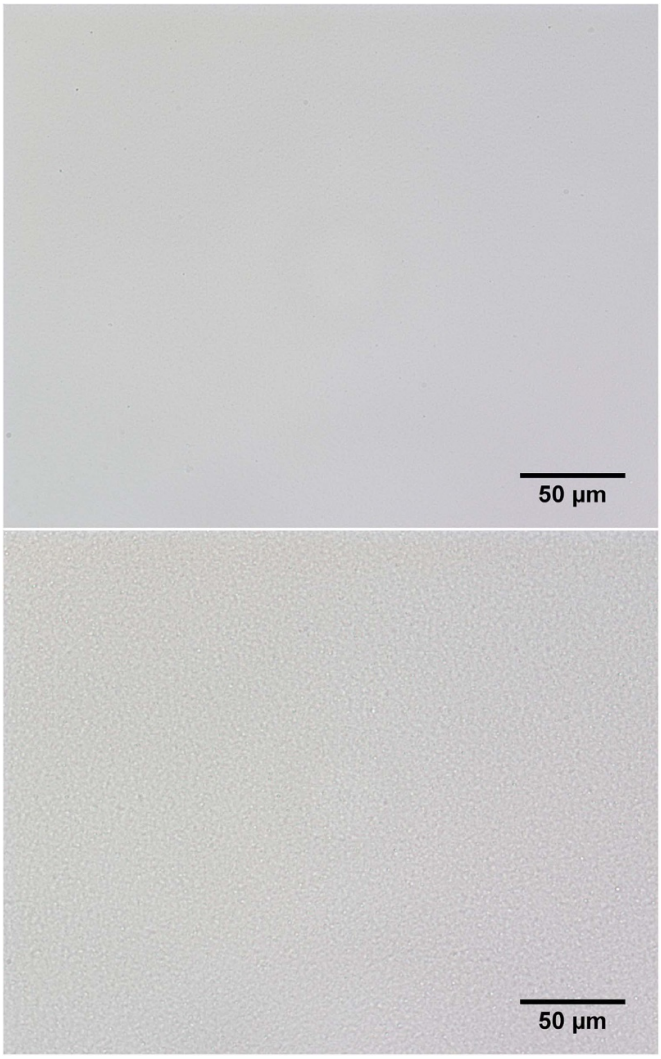

Figure 7. Microscopy pictures of upper (top) and lower (bottom) phase of guar gum dissolved in milk taken with bright field microscopy and a magnification of 400×.

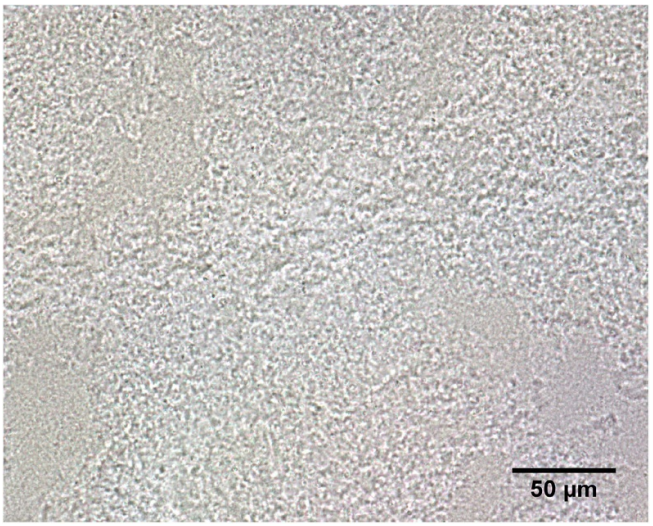

Figure 8. Microscope image of gellan gum in milk taken with bright field microscopy and a magnification of 400×.

Microscope images were also taken for dried samples (droplet evaporation). These images revealed a clearer picture than the images of the wet samples. Figure 10 shows a picture of a dried droplet of pure

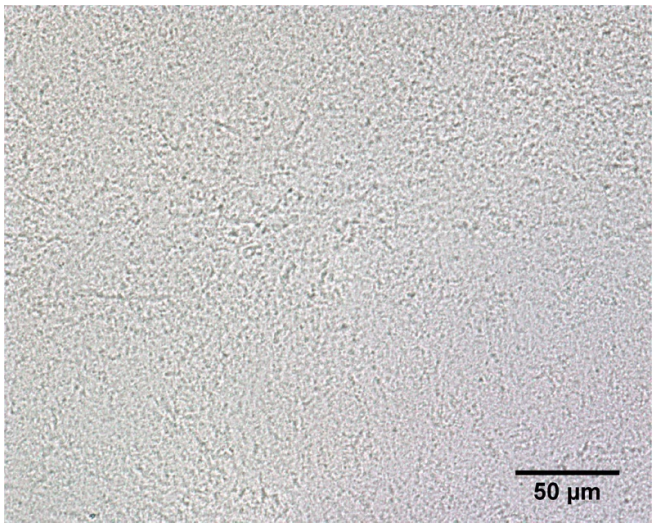

Figure 9. Microscope image of iota-carrageenan in milk taken with bright field microscopy and a magnification of 400×.

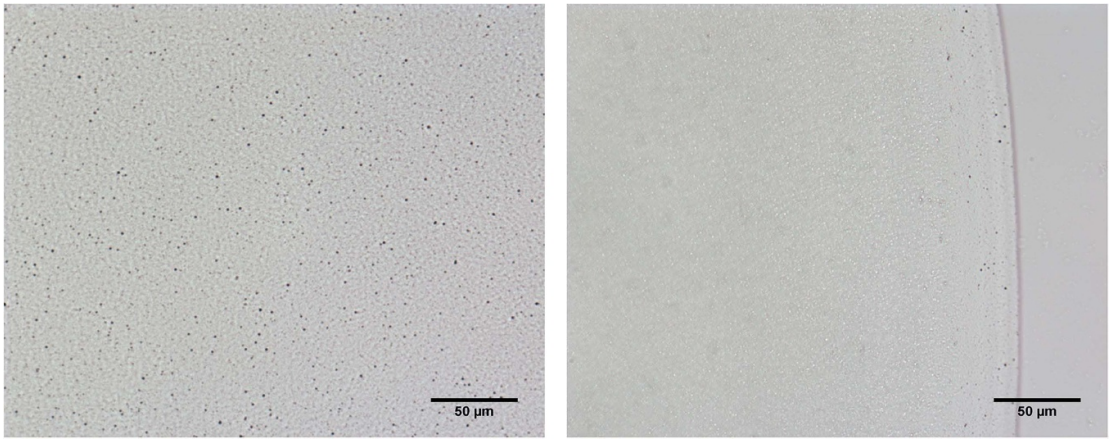

Figure 10. Microscope images of a dried droplet of pure skimmed *Heumilch* taken with bright field microscopy at a magnification of 400× in the middle of the sample (left) and at the edge of the droplet (right).

skimmed *Heumilch*. Tiny black spots could be seen throughout the whole sample. On the right side of figure 10 an image including the edge of the droplet is shown in the same magnification, where the edge of the milk droplet was focused.

A network could be seen in the upper phase of the xanthan gum sample, which was most likely formed by the hydrocolloid itself. Several xanthan gum molecules are forced to contract with respect to each other into a network while drying. Thus, a link of the network in the dried sample is formed by several xanthan gum molecules. The network could be seen throughout the whole sample. The shape of the meshes and the mesh size was only slightly varying between the interior and the edge of the dried droplet. In the lower phase a large network shred was found in the middle surrounded by some smaller ones. Other than that the image looked like the image of the dried droplet of pure milk - only tiny black spots throughout the whole sample. The droplets were taken from the sample with a pipette. Especially for the lower phase it was very difficult to clearly separate the two phases. When taking the droplet from the lower phase the pipette tip had to go through the upper phase. So it could not be prevented that small parts of the upper phase stick to the pipette tip and finally appear in the droplet for the lower phase. Still, these images show clearly that (at least most of the) xanthan gum was in the upper phase, whereas most of the milk constituents were present in the lower phase. Figure 11 shows microscope images of dried droplets of upper as well as lower phase of xanthan gum in milk.

For guar gum a similar result was obtained. In this case a network structure could be seen in the upper phase as well. However, this network structure had a different appearance than in the case of xanthan gum. Towards the edge of the dried droplet the guar gum network structure looked stretched and very close to the

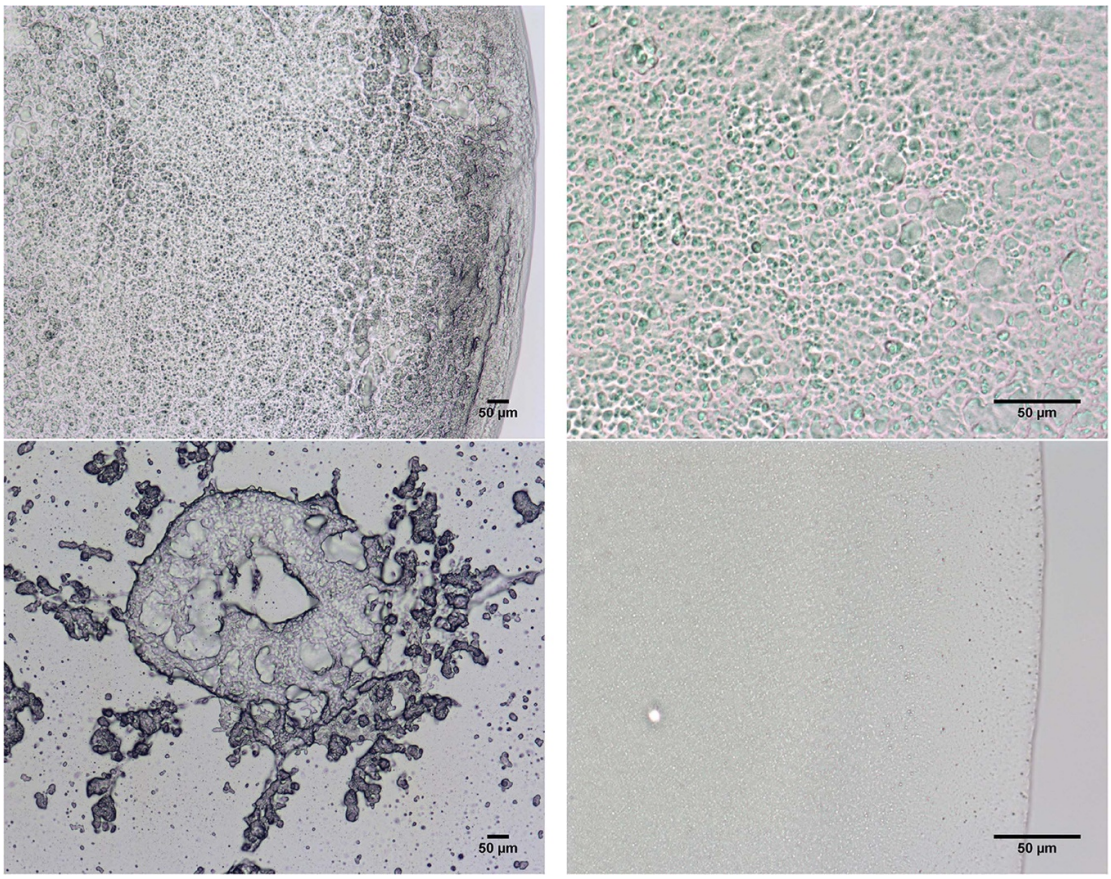

Figure 11. Microscope images of dried droplets of xanthan gum in milk. Top: upper phase with a magnification of 100× (left) and 400× (right). Bottom: lower phase with a magnification of 100× (left) and 400× (right).

edge, the meshes of the network were smaller than in the interior of the droplet. This behaviour can be explained by the internal flexibility of the guar gum molecule. At the outer edge the droplet is drying faster and the gum forms small meshes by entangling while drying. Towards the middle the droplet becomes thicker and is thus drying slower. One part of the guar gum molecule is already stuck to the surface of the microscope slide since it is dry already, whereas the other part of the molecule is still in the liquid. The gum is attracted by the water. While drying, the guar gum molecule is stretched. The lower phase looked very similar to the pure milk sample. There were tiny black spots throughout the whole dried droplet. The only difference was that the black spots in the middle appeared to be slightly larger and there were a few larger oval shapes which were probably traces from the upper phase or an air bubble. Again, the sample was taken with a pipette and by that it could not be prevented completely that tiny amounts of the upper phase occurred in the droplet for the lower phase. Still, these pictures revealed clearly that guar gum molecules were present in the upper phase and most of the milk constituents were in the lower phase. The corresponding pictures are shown in figure 12.

Microscope images of the dried droplet of skimmed *Heumilch* with iota-carrageenan are shown in figure 13. The picture with a magnification of 100× showed wormlike structures throughout the whole sample. The 400× picture looked similar to the microscope image of the wet iota-carrageenan milk droplet. Tiny black spots could be seen throughout the whole sample suggesting that the milk components were distributed throughout the whole sample. The other (wormlike) structures must have been caused by the iota-carrageenan molecules.

The gellan gum milk sample which is shown in figure 14 looked like a ruptured network. Network fragments could be seen throughout the whole sample. The network structure is caused by the gellan gum when it dries and is contracted during the drying process. The rupture of the network structure can also be explained by the drying process. While the droplet is shrinking parts of the network are dried already and thus fixed on the surface of the microscope slide while other parts of the molecules are still in the liquid of the droplet. In comparison to the xanthan gum and guar gum sample where the network was not ruptured there is more water available in the gellan gum sample because no phase separation occured.

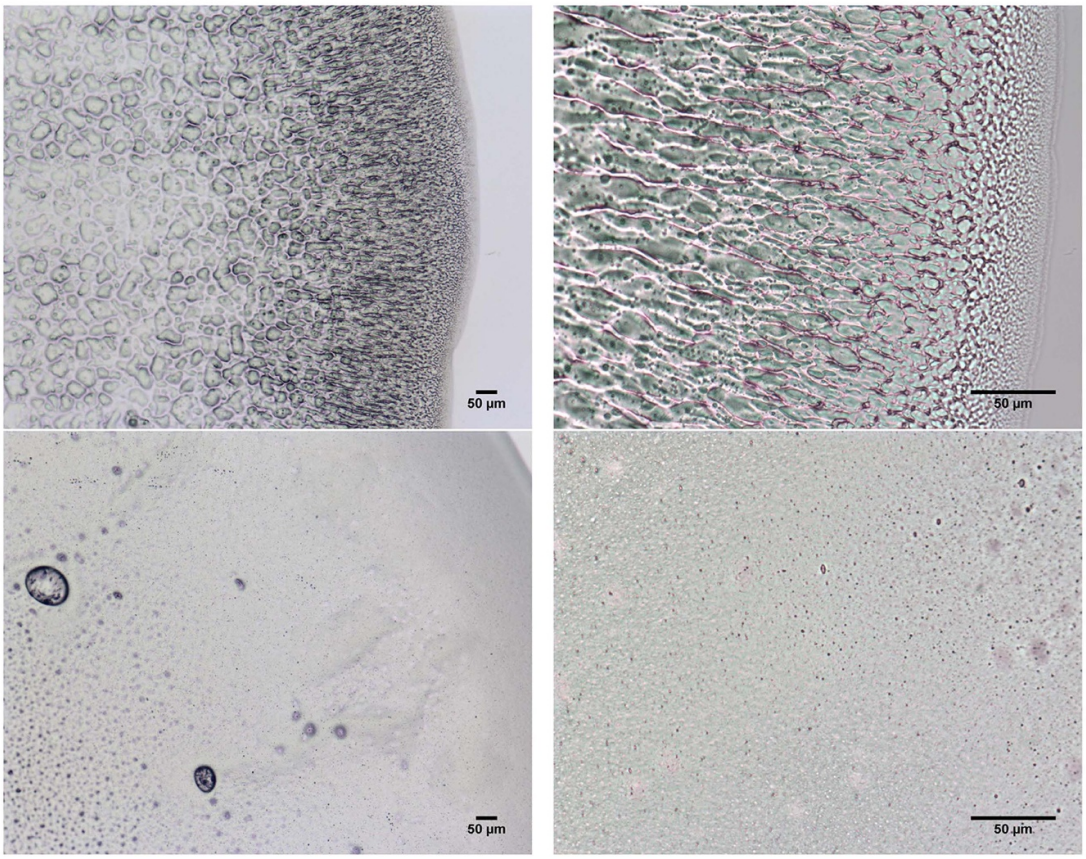

Figure 12. Microscope images of dried droplets of guar gum in milk. Top: upper phase with a magnification of 100× (left) and 400× (right). Bottom: lower phase with a magnification of 100× (left) and 400× (right).

3.4. Zetasizer

Zeta potential measurements were performed to learn about the charges of the different hydrocolloids and to study their influence on the milk system. Table 2 summarizes the zeta potential values of the different hydrocolloids dissolved in milliQ water, in milliQ water with whey protein and in milk. Shown are mean values of the measurements. The values for the zeta potential of pure skimmed milk were between −24 mV and −27 mV depending on the package of milk. Therefore, it could be concluded that the values of upper and lower phase of guar gum in milk as well as of the lower phase of xanthan gum in milk were in the range of pure milk samples. The casein micelles in milk are negatively charged and were probably measured by the zetasizer. However, there are whey proteins with positive as well as negative surface charges, salts and ions present in milk as well. Zeta potential values are always relative values and do not show the actual charge of the particle. Besides the actual charge of the particle and the screening the zeta potential value also depends on the suspension medium. Thus, the values of hydrocolloids dissolved in milk and those of hydrocolloids in milliQ water cannot be directly compared to each other. In both cases the solvent will be water but in milk there are many more other particles and ions present than in milliQ water.

Xanthan gum is the most negatively charged compared to the other three hydrocolloids. When whey protein was added, the measured particles were negatively charged. In milk the value of the lower phase was in the range of pure skimmed milk. For the upper phase of xanthan gum in milk the Malvern Zetasizer Nano-Z measured two values for most of the measurements. One of which was in the range of milk, but the other one was stronger negatively charged. The value that is stronger negatively charged may indicate that there is a higher content of xanthan gum in the upper phase.

Guar gum consists entirely of polar monomers and is not charged. So no charge could be measured by the zetasizer. For the case of guar gum and whey protein dissolved in milliQ water a negative zeta potential was measured which must be caused by the whey protein. For the case of only whey protein dissolved in milliQ water similar values were measured. All guar gum dissolved in milk values were in the range of the zeta potential values of milk. Therefore it could be concluded that the measured values were caused by the casein micelles or whey proteins since guar gum is an uncharged molecule. For the case of guar gum dissolved in milk a phase separation could be observed after a few hours. Here the particles measured in

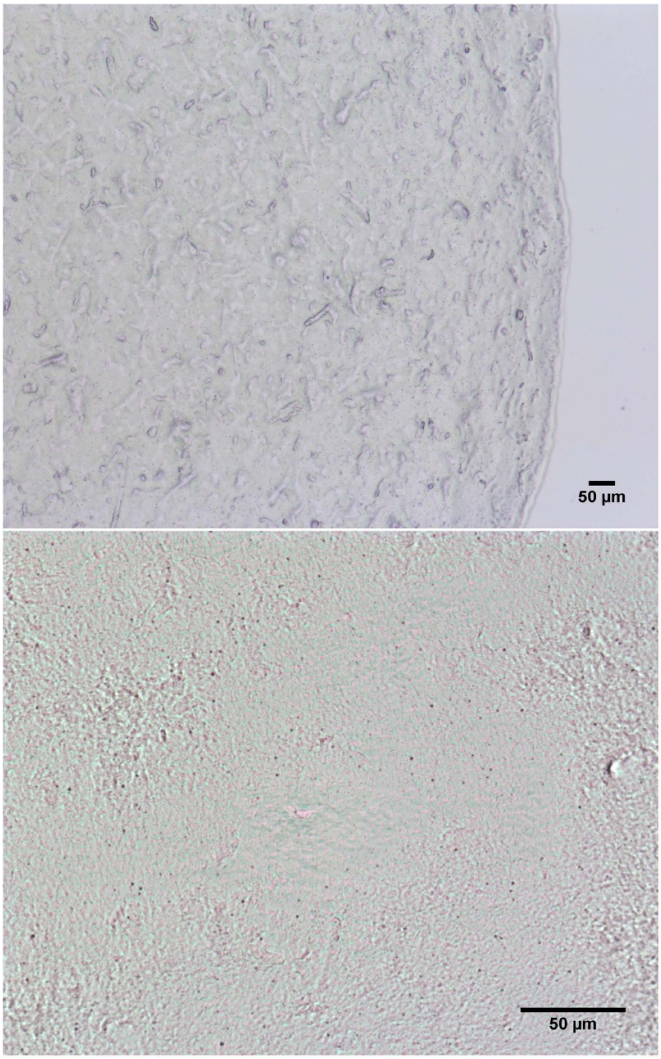

Figure 13. Microscope images of dried droplets of iota-carrageenan in milk with a magnification of 100× (top) and 400× (bottom).

milk - casein micelles and whey proteins - seemed to be present in both, upper and lower phase. However, the zeta potential measurement did not indicate whether the concentration of the measured particles decreased or increased in one of those phases.

Iota-carrageenan is negatively charged, but less strongly than xanthan gum and gellan gum. The measured values for the case of iota-carrageenan dissolved in milliQ water scattered more than for the other samples. A reason could be that Iota-carrageenan in water solutions were very clear even at higher concentrations. Because of the non-reproducibility of the results no mean values were calculated. The value for iota-carrageenan dissolved in milk was with (-27.5 ± 3.7) mV in the range of the corresponding milk value (-25.2 ± 5.2) mV.

Looking at the gellan gum data no difference between the pure gellan gum dissolved in milliQ water sample and the gellan gum + whey protein dissolved in milliQ water sample could be discovered. When comparing the values of the different hydrocolloids dissolved in milliQ water gellan gum was less negatively charged than xanthan gum but more negatively charged than iota-carrageenan. The value of gellan gum in milk was slightly more negatively charged (-31.0 ± 5.6) mV than the corresponding pure milk sample (-25.2 ± 5.2) mV. But considering the standard deviation it was still in the range of milk.

3.5. Atomic force microscope

AFM images of the hydrocolloids dissolved in milliQ water were taken to investigate the stiffness and size of the different hydrocolloids. Furthermore, the purpose of interpreting AFM images of the hydrocolloids dissolved in milk was to give information about their behaviour in milk and their interaction with the milk constituents.

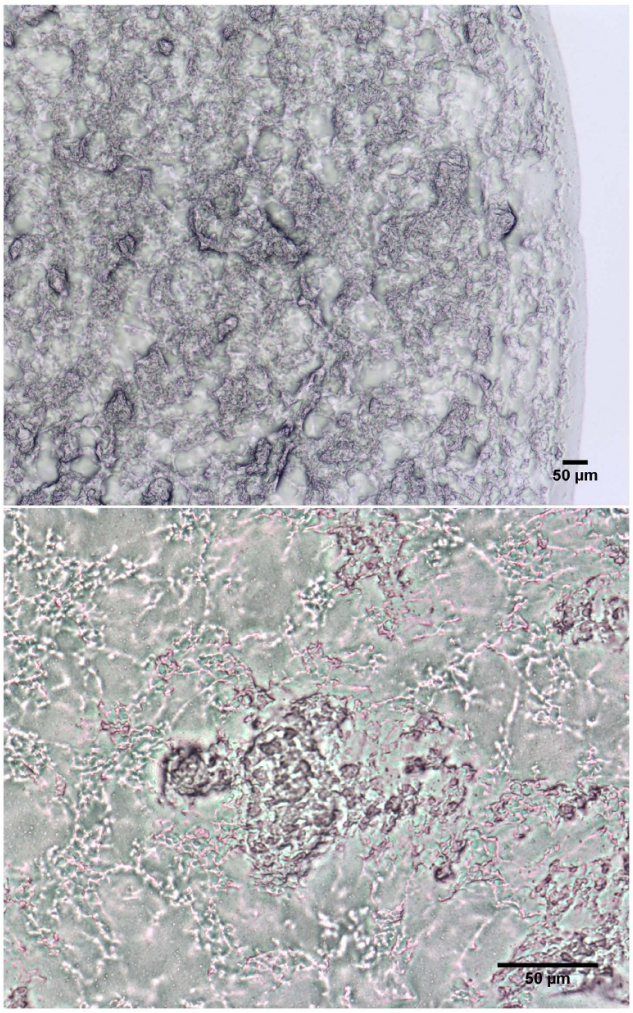

Figure 14. Microscope images of a dried droplet of gellan gum in milk with a magnification of 100× (top) and 400× (bottom).

Table 2. Summary of zeta potential measurement results. The shown values are mean values. HC stands for hydrocolloid and WP for whey protein.

	Xanthan gum [mV]	Guar gum [mV]	Iota-carrarrageenan [mV]	Gellan gum [mV]
HC	-75.0 ± 5.6	–		-56.3 ± 4.5
HC + WP	-62.4 ± 6.0	-32.1 ± 7.0		-56.1 ± 4.4
HC + milk			-27.5 ± 3.7	-31.0 ± 5.6
Upper phase	-26.2 ± 4.7 -37.6 ± 3.8	-24.4 ± 6.6	–	–
Lower phase	-25.0 ± 5.4	-25.1 ± 5.8	–	–

For the hydrocolloids dissolved in milliQ water samples were prepared using two different methods: a droplet of sample solution was either dried using an argon stream or the droplet evaporated underneath a glass cover. For the same sample the two preparation methods resulted in very different behaviour of the hydrocolloids. The evaporated samples looked much stiffer than the argon dried ones for each of the hydrocolloids, respectively. Figure 15 shows an argon dried and a droplet evaporated xanthan gum dissolved in milliQ water sample in comparison.

To learn about the stiffness and to compare the different hydrocolloids, the argon dried samples were used, because the evaporated samples may have been influenced by the mica surface. So the images of the argon dried samples probably gave the more natural picture.

In figure 16 an AFM image of an argon dried sample is shown for each of the hydrocolloids.

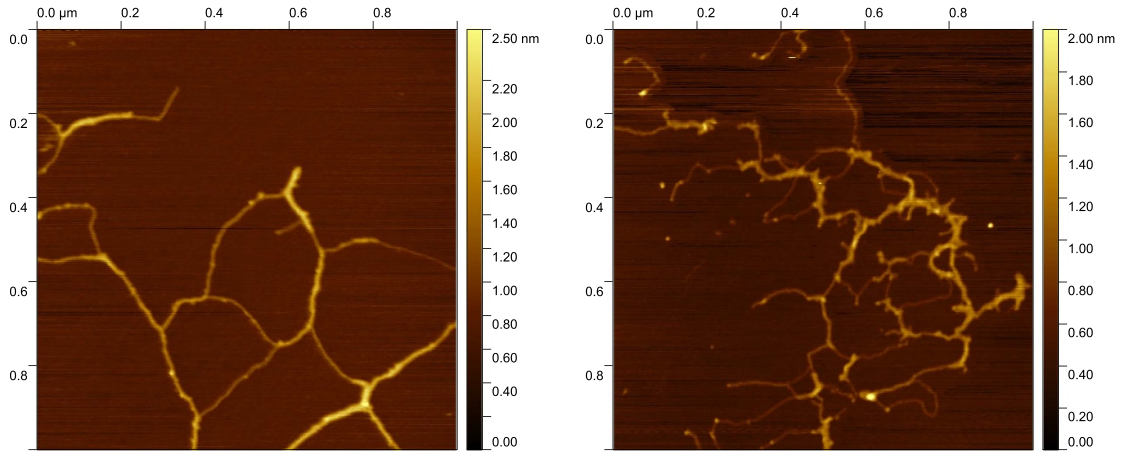

Figure 15. AFM images of an evaporated droplet of xanthan gum in milliQ water (left) and an argon dried xanthan gum in milliQ water sample (right). The sample concentration before drying was 1 μg g^{-1}.

Looking at the AFM images of argon dried hydrocolloid dissolved in milliQ water samples, it was stated that xanthan gum is the most rigid one. There were probably several xanthan gum molecules displayed in the picture. Separating strands of xanthan gum showed branch-like structure. Between those connection points the strands looked pretty straight and thus stiff. Loops were very rare.

If the xanthan gum molecules are modelled as stiff rods for simplicity, their length can be estimated using the chemical structure of the molecule and the measured molar mass. The mass of one monomer of a xanthan gum molecule can be calculated after counting all carbon atoms, oxygen atoms and hydrogen atoms in a monomer:

$$m_{mono,XG} = 35m_C + 29m_O + 50m_H \approx 1.55 \cdot 10^{-21}\,\mathrm{g} \tag{1}$$

where $m_C = 12.01\,\mathrm{u}$ is the mass of one carbon atom, $m_O = 16.00\,\mathrm{u}$ the mass of one oxygen atom and $m_H = 1.01\,\mathrm{u}$ the mass of one hydrogen atom. The atomic mass unit u is given by $1\,\mathrm{u} = 1.66 \cdot 10^{-27}\,\mathrm{kg} = 1.66 \cdot 10^{-24}\,\mathrm{g}$. The length of one monomer is $L_D = 0.94\,\mathrm{nm}$ [40]. Using the mean value of the measured molar mass of xanthan gum $M_{W,XG} = 1496500\,\mathrm{g\ mol^{-1}}$ the number of monomers in one polymer can be calculated as:

$$N_{mono,XG} = \frac{m_{XG}}{m_{mono,XG}} = \frac{M_{W,XG}}{N_A m_{mono,XG}}$$

where m_{XG} is the mass of a xanthan gum molecule, $m_{mono,XG}$ the mass of one xanthan gum monomer and $N_A = 6.022 \cdot 10^{23}\ \mathrm{mol^{-1}}$ is the Avogadro constant. It follows for the length of the xanthan gum molecules:

$$L = NL_D = \frac{M_{W,XG}}{N_A m_{mono}} L_D \approx 1.51\ \mu\mathrm{m}$$

Thus, the length of one xanthan gum rod is much larger than the diameter of a casein micelle which is about 130 nm.

Guar gum appeares as most flexible. The chains can be thus assumed to perform a random walk confined to two dimensions (in projection) during drying. Neighbouring chain segments had random orientation. The expected size of such a random walk can be estimated using equations from polymer physics. A real chain performs a self-avoiding walk. Its mean square average end-to-end distance is estimated in the scaling limit by simple Flory arguments to be:

$$R_F \cong N^{3/5} a \tag{2}$$

where N is the number of segments and a is the lengths of one segment of the random walk [5]. In order to consider the stiffness of the molecule the length a is not defined by one monomer but by a few monomers. a describes the length of straight freely jointed effective bonds (Kuhn length) [41]. The relationship between the average end-to-end distance R_0 and the radius of gyration R_g of the molecule is given by:

$$\langle R_g^2 \rangle = \frac{Na^2}{6} = \frac{\langle R_0^2 \rangle}{6} \tag{3}$$

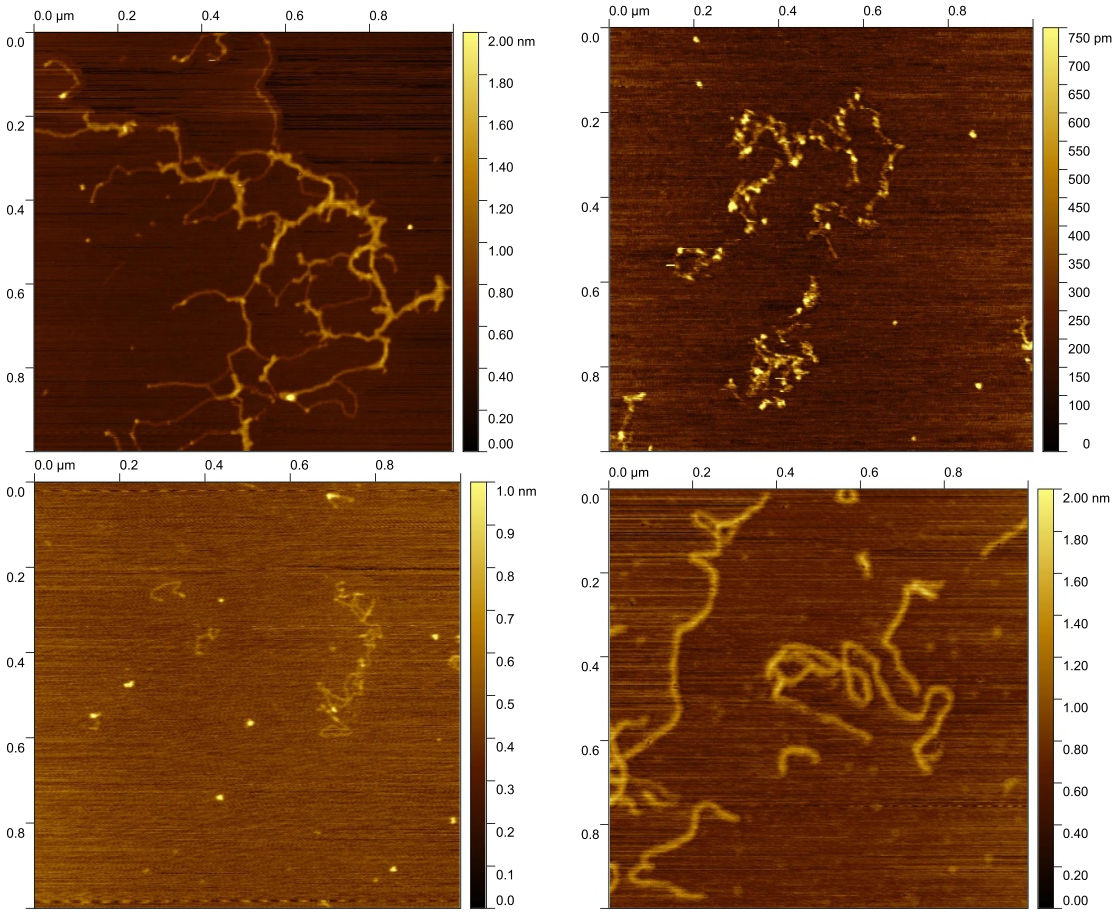

Figure 16. Comparison of the different hydrocolloids: AFM images of argon dried samples with a concentration of 1 μ g/g and a scan size of 1 μm. Upper left: xanthan gum. Upper right: guar gum. Lower left: iota-carrageenan. Lower right: gellan gum.

[41]. The mass of a guar gum monomer can be calculated from its chemical structure:

$$m_{mono,G} = 18m_C + 15m_O + 30m_H = 8.08 \cdot 10^{-22}\,\mathrm{g}$$

where $m_C = 12.01\,\mathrm{u}$ is the mass of a carbon atom, $m_O = 16.00\,\mathrm{u}$ is the mass of an oxygen atom and $m_H = 1.01\,\mathrm{u}$ is the mass of a hydrogen atom. The atomic mass unit u is given by $1\,\mathrm{u} = 1.66 \cdot 10^{-27}\,\mathrm{kg} = 1.66 \cdot 10^{-24}\,\mathrm{g}$. The molar mass of guar gum was measured to be $M_{W,G} = 1612667\,\mathrm{g\,mol^{-1}}$. The number of monomers can thus be calculated:

$$N_{mono,G} = \frac{M_{W,G}}{N_A m_{mono,G}} \tag{4}$$

where N_A is the Avogadro constant. The length of a disaccharide is approximately $L_D = 0.94$ nm [40], which will be used to approximate the length of one monomer L_{mono}. When calculating the dimensions of a random walk of a polymer the Kuhn length is used to approximate the length a of the random walk. The Kuhn length considers the stiffness of the polymer molecule. Thus, $a = kL_{mono}$ where k is a natural number and L_{mono} is the length of a monomer. The number of Kuhn segments N of the random walk becomes $N = \frac{N_{mono}}{k}$. It follows from equations (2) and (3):

$$R_g \sim \frac{1}{\sqrt{6}} R_F \approx \frac{1}{\sqrt{6}} a N^{3/5} \approx \frac{1}{\sqrt{6}} k L_{mono} \left(\frac{N_{mono,G}}{k}\right)^{3/5} \tag{5}$$

Table 3 summarizes calculated values for the radius of gyration R_g for a guar gum molecule for different k values.

It was not known how many random walks of guar gum molecules were seen in the AFM image in figure 16 (upper right) since they may aggregate during drying, but the obtained values seemed to be a good first estimation for the size of the random walks performed by guar gum molecules.

Table 3. Estimated values for the radius of gyration R_g of a guar gum molecule in dependence of the Kuhn length which is defined by the number of monomers k in one Kuhn segment.

k	R_g [nm]
1	49.7
2	65.6
3	77.1
4	86.5
5	94.6

Also iota-carrageenan appeared very flexible, as expected. The chain was performing a random walk as well. However, the random walk coil seemed to be stretched. The stretching can be explained by the negative charge of the molecule (cf polymer physics of a chain under traction). Gellan gum looked stiffer than iota-carrageenan but it showed loops so it could be considered to be more flexible than xanthan gum. This behaviour can be explained by its negatively charged backbone and the uncharged side chains. The zeta potential measurements suggested that gellan gum was more negatively charged than iota-carrageenan but less negatively charged than xanthan gum. Additionally, the short uncharged side chains cause a small steric hindrance.

Furthermore, AFM images were taken for the hydrocolloids dissolved in milk. Figure 17 shows AFM images of upper as well as lower phase of xanthan gum dissolved in milk. For each of the phases two images with different scan size and from different samples are displayed.

In the upper phase thin rod-like structures were recognized that were similar to the ones seen for the xanthan gum molecules in figure 16 (upper left). This observation suggested that xanthan gum was mainly dissolved in the upper phase. Besides these structures there were also spherical particles seen. In the upper left picture of figure 17 these particles seemed to connect the rods. A network was formed. At the connection points of the rod-like structures the spherical shapes were deformed. They got stretched or took triangle-like shapes. In the image displayed on the upper right hand side of figure 17 it appeared more like the rod-like structures were stretched out and the spherical shaped particles were evenly distributed. They were connected with the rods but were also everywhere in between the rods. In figure 17 (upper left) the more or less sphere-like particles had sizes of less than 26 nm up to 75 nm and a height of up to 5 nm. In figure 17 (upper right) the sizes ranged from about 10 nm up to 38 nm and had a height of up to 6 nm. These sizes were measured using the software Gwyddion. For more information on the measurement see the appendix. At least the smaller particles were most-likely whey proteins. The larger ones could have been agglomerates of whey proteins since they were too small to be intact casein micelles. Whey proteins have positive as well as negative surface charges. Thus, an interaction between the positive surface charges of whey proteins with the negative charged xanthan gum rods could be possible. This behaviour could explain the network structure in figure 17 (upper left).

Besides the small spherical particles which were observed in the lower phase as well, also large spheres were detected. Two examples are shown in figure 17 (lower left and lower right). Due to their size and shape these larger spheres could have been casein micelles, which would suggest that (most of the) casein micelles were found in the lower phase. The sphere in figure 17 (lower left) had a horizontal diameter of 133.8 nm and a vertical diameter of 146.5 nm. The height was about 30.0 nm. The shape of a sphere stuck to the mica surface can be approximated by half an ellipsoid. From this information a volume of

$$V = \frac{1}{2} V_{ellipsoid} = \frac{2}{3}\pi abc \approx 307,\ 902.8\ \text{nm}^3 \approx 0.3 \times 10^6\ \text{nm}^3 \tag{6}$$

with a, b, and c the semiaxis of the ellipsoid, can be calculated. A casein micelle (CM) with a diameter of 130.0 nm would have a volume of

$$V_{CM} = V_{sphere} = \frac{4}{3}\pi r^3 \approx 1,\ 150,\ 346.5\ \text{nm}^3 \approx 1.2 \times 10^6\ \text{nm}^3 \tag{7}$$

One reason for the lower volume of the casein micelle detected by AFM compared to the theoretical volume is that the arms of the κ-casein (hairy layer of the casein micelle) were probably not extended in the dried version. Another reason is that the casein micelle was dried. The submicelles in the inner part of the casein micelle are quite loose. While drying-out the volume thus got smaller and the height of the micelle in the AFM image decreased.

The sphere in the second picture (figure 17 (lower right)) had a horizontal diameter of 180.7 nm and a vertical diameter of 186.5 nm. Its height was about 70.0 nm. From that a volume of

$$V = \frac{1}{2} V_{ellipsoid} = \frac{2}{3}\pi abc \approx 1,\ 235,\ 189.7\ \text{nm}^3 \approx 1.2 \times 10^6\ \text{nm}^3 \tag{8}$$

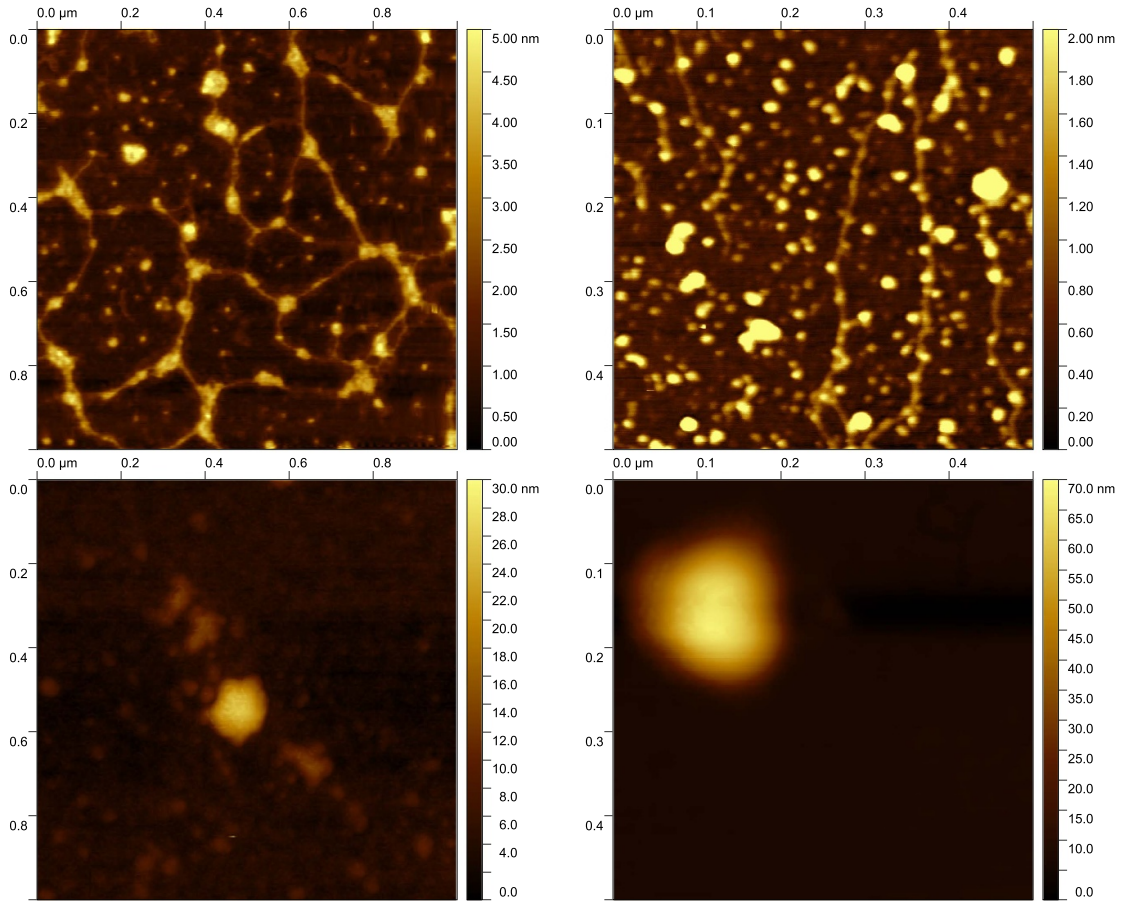

Figure 17. AFM images of upper phase (top) as well as lower phase (bottom) of xanthan gum dissolved in milk.

could be calculated which comes very close to the theoretical volume of a casein micelle. Since there were small as well as large spheres seen in the lower phase, it could be concluded that there were casein micelles as well as whey proteins in the lower phase. It could not be excluded that there were xanthan gum molecules in the lower phase. In case there were xanthan gum molecules in the lower phase these thin molecules with a height of only 1−2 nm could not be distinguished besides the large casein micelles with a height of up to 70 nm.

Figure 18 shows pictures of upper and lower phase of guar gum dissolved in milk.

In the upper phase a lot of small particles were seen. These spheres had a size of 20 nm (or even less) to 33 nm (cf appendix) and a height of less than 6 nm. These spheres probably represented whey proteins. In the lower phase there were much larger spheres. The largest one had a horizontal diameter of 291 nm and a vertical diameter of 318 nm. Its height was about 40 nm. These parameters led to a volume of

$$V = \frac{1}{2} V_{ellipsoid} = \frac{2}{3}\pi abc \approx 1,938,111 \text{ nm}^3 \approx 1.9 \times 10^6 \text{ nm}^3 \tag{9}$$

which is slightly larger than the theoretical value for the volume of a casein micelle, but still in the range of estimation and its error. As mentioned before the theoretical value for a casein micelle (CM) with a diameter of 130.0 nm is $V_{CM} = V_{sphere} = \frac{4}{3}\pi r^3 \approx 1,\ 150,\ 346.5 \text{ nm}^3 \approx 1.2 \times 10^6 \text{ nm}^3$. On the other hand, a natural variation in the size of casein micelles is expected as stated in different references e.g. by P.F. Fox in [42]. Another sphere measured had a horizontal diameter of 160 nm and a vertical diameter of 188 nm. Its height was only about 30 nm. These values led to a volume of

$$V = \frac{1}{2} V_{ellipsoid} = \frac{2}{3}\pi abc \approx 472,496 \text{ nm}^3 \approx 0.5 \times 10^6 \text{ nm}^3 \tag{10}$$

which is a bit smaller than a casein micelle. An explanation for being smaller than the expected value is given by the drying out of the micelle even in its internal part. In any case, it had to be stated that there were much larger spheres in the lower phase than in the upper phase. Guar gum molecules were only detectable in aqueous solution at an AFM image height of 750 pm (cf figure 16 (upper right)). Dissolved in milk, guar

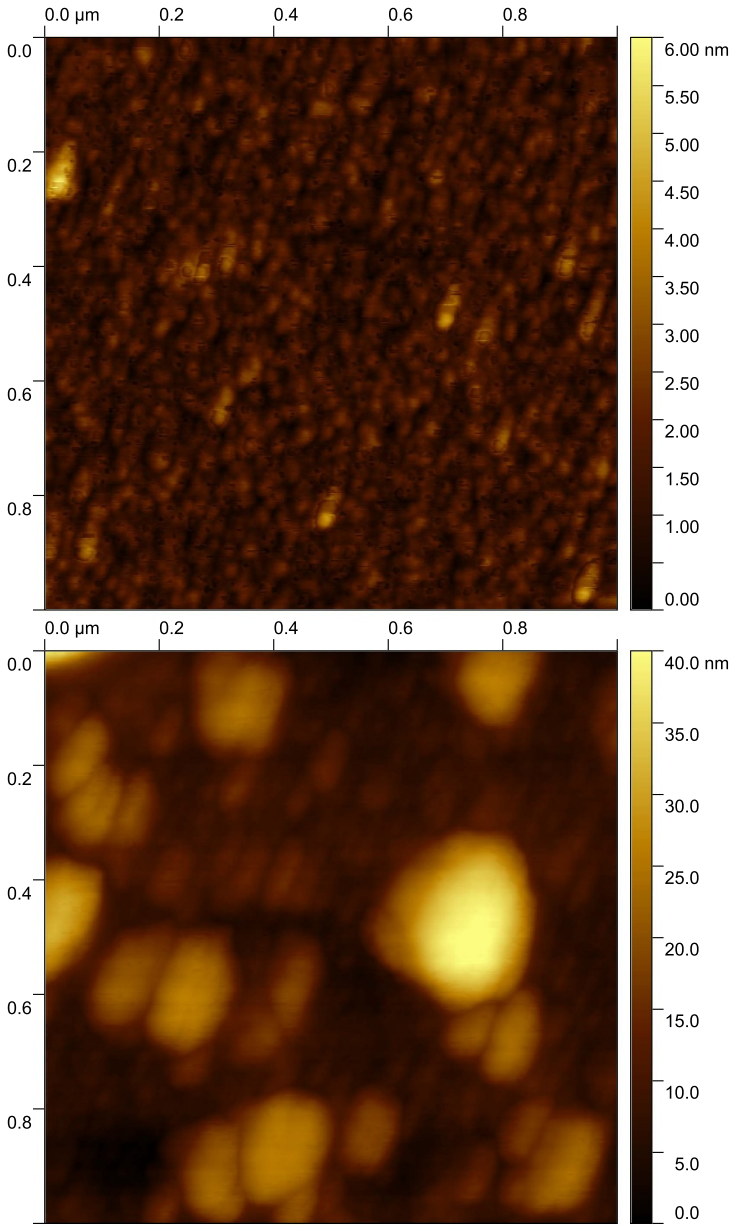

Figure 18. AFM images of upper phase (top) and lower phase (bottom) of guar gum dissolved in milk.

gum molecules were not visible next to the large milk proteins, probably due to their very thin chain segments. The images of guar gum dissolved in milk (cf figure 18) had heights of 6 nm respectively 40 nm which was much larger. Nevertheless, the fact that most of the casein micelles were observed in the lower phase indicates that they were depleted by the guar gum molecules and that these were thus present in the upper phase. Further measurements will have to confirm the presumption that depletion interaction [24, 43] is one of the driving forces for the phase separation and why guar gum is found in the upper phase.

For iota-carrageenan and gellan gum dissolved in milk, AFM images looked similar to those of pure milk. An AFM image of iota-carrageenan in milk is shown in figure 19. Figure 20 displays an AFM image of gellan gum dissolved in milk. These hydrocolloids did not show a macroscopic phase separation. The hydrocolloids themselves could not be seen due to the scale of the image, since the hydrocolloids were very small (height of about 1 to 2 nm) compared to the larger particles with a height of 25 nm or 35 nm, respectively, and thus could not be displayed in the same picture. So only the larger milk constituents could be seen. The larger particles in the picture were a bit too small to be casein micelles. Reasons why the casein micelles in the AFM images could be smaller than the ones in liquid have been discussed before. In case gellan gum respectively iota-carrageenan, complex formation with whey proteins could be another explanation for the larger particles which have been observed.

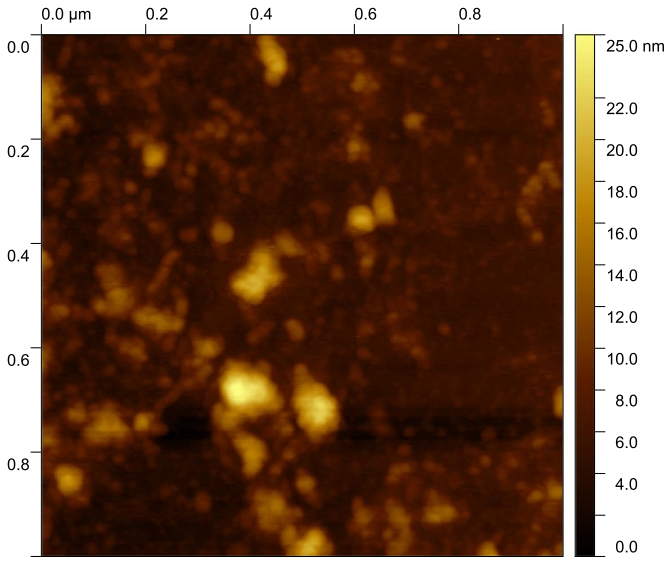

Figure 19. AFM image of iota-carrageenan dissolved in milk.

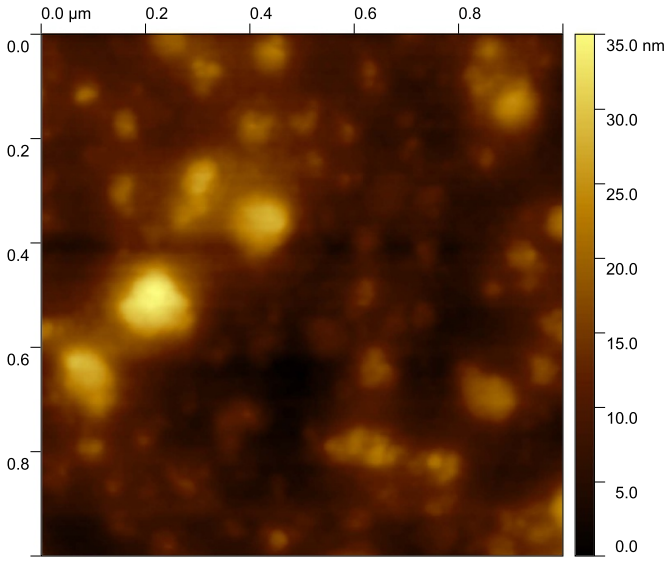

Figure 20. AFM image of gellan gum dissolved in milk.

3.6. Particle size analyser

Particle sizes were measured in order to confirm the results and to find out whether complexes were formed, especially in the case of iota-carrageenan and gellan gum, where the AFM images looked like milk and the zeta potential values were only slightly shifted but still in the range of pure milk. Using static light scattering it was possible to investigate the wet systems. However, the non-spheric shape of some of the particles could not be taken into account. Figure 21 shows the upper phase and lower phase of xanthan gum in milk, pure skimmed milk and xanthan gum in milliQ water.

For xanthan gum in water two peaks could be seen, one at a particle size of 53 nm and one at 598 nm. Probably these results were caused by the non-sphericity of the xanthan gum molecules.

For pure milk three peaks were measured. The first peak, representing a particle size of 58 nm, was probably caused by whey proteins although such a size is quite large for whey proteins. However, the expected size of a whey protein would have been smaller than the lower resolution limit of the particle size analyser which was 40 nm. Thus the deviation might have been caused by a reduced accuracy close to the lower resolution limit. The second peak at 134 nm was probably caused by the casein micelles since it fitted the theoretical size of a casein micelle (sphere with diameter 130 nm) very well. The third peak at 311 nm was of unclear origin. It could have been caused by little fat droplets. After centrifugation the milk had been

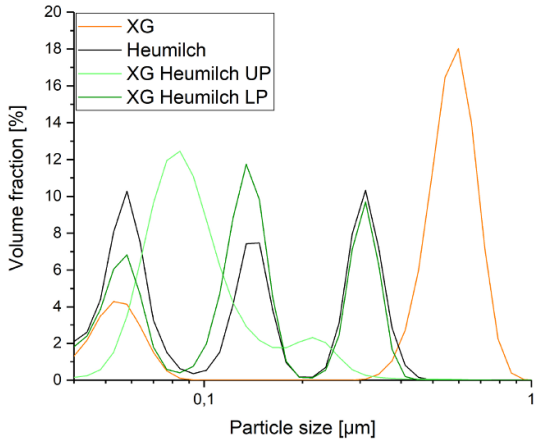

Figure 21. Particle sizes of xanthan gum, xanthan gum in milk (upper and lower phase) and pure milk.

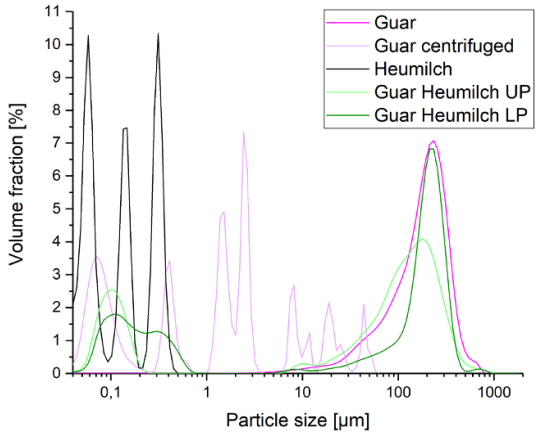

Figure 22. Particle sizes of guar gum, guar gum in milk (upper and lower phase) and pure milk.

filtered using syringe filters. The smallest filter that had been used had a pore size of 0.8 μm. Therefore, no larger particles should have been seen in the milk sample which indeed has been the case according to the particle size measurement. However, small fat droplets might have still been in the milk after centrifugation. Centrifugation was performed at a speed of 6,424$\times$ g. The density of the fat droplets is $\rho_{fat} = 0.9$ g ml^{-1}. For the whey a density of $\rho_{whey} = 1.0$ g ml^{-1} was approximated. For a fat droplet with a diameter of 311 nm the gravitation would be

$$F_G = \frac{4}{3}\pi R^3 \rho_{fat} a = 8.9 \cdot 10^{-13}\ \text{N} \approx 0.9\ \text{pN} \tag{11}$$

and the buoyant force would read

$$F_B = \frac{4}{3}\pi R^3 \rho_{whey} a = 9.9 \cdot 10^{-13}\ \text{N} \approx 1.0\ \text{pN} \tag{12}$$

where R is the droplet radius and a is the acceleration of the centrifuge. Since $F_B > F_G$ the particle would cream. The friction force F_F can be used to calculate the velocity of the creaming droplet. It holds:

$$F_G + F_F = F_B \tag{13}$$

$$F_F = F_B - F_G \tag{14}$$

With

$$F_F = 6\pi\eta R v \tag{15}$$

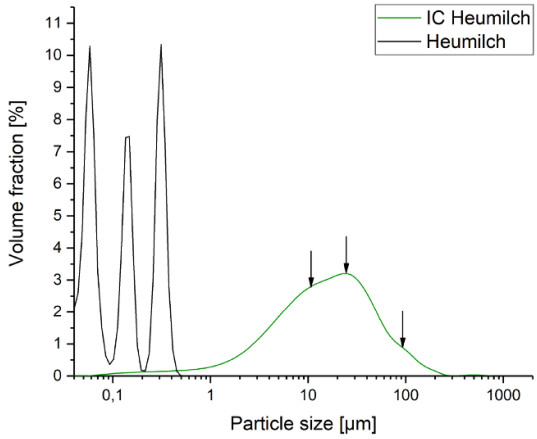

Figure 23. Particle sizes of iota-carrageenan in milk and pure milk. The arrows mark bumps inside a broad peak.

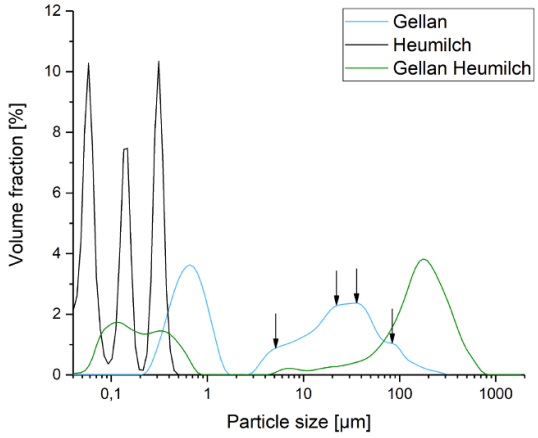

Figure 24. Particle sizes of gellan gum, guar gum in milk and pure milk. The arrows mark bumps inside a broad peak.

where η is the viscosity of the whey and v is the particle's velocity. It follows:

$$v = \frac{2}{9\eta} R^2 a(\rho_{whey} - \rho_{fat}) = 3.3 \cdot 10^{-8}\ \mathrm{m\ s^{-1}} \tag{16}$$

The dynamic viscosity of whey is between 800–1500 mPa s [44]. For the calculation it was approximated with 1 Pa s. If a uniformly accelerated motion is assumed, time and path can be calculated:

$$v = at \qquad \Rightarrow \qquad t = \frac{v}{a} = 5.4 \cdot 10^{-13}\ \mathrm{s}$$

$$s = \frac{1}{2} a t^2 = 9.1 \cdot 10^{-21}\ \mathrm{m} = 9.1 \cdot 10^{-12}\ \mathrm{nm} \tag{17}$$

This result means that the fat droplet was moving only very little and would not have reached the surface during centrifugation. Fat droplets of such a size would still be distributed throughout the milk.

For the lower phase of xanthan gum in milk three peaks were measured. These three peaks were located at the same particle sizes as the peaks of the pure milk sample. This clearly represented that milk constituents were in the lower phase, which is in accordance with the other measurements performed and described before. The two peaks of the upper phase of xanthan gum in milk (at 84 nm and 214 nm) did not fit with any of the other peaks - neither the pure milk sample nor the xanthan gum in water sample. This behaviour could be explained by whey proteins binding to a xanthan gum molecule and thus making it slightly more flexible.

The results of the particle size measurements of guar gum are displayed in figure 22. Guar gum is produced from guar pods that are ground. In the powder there are still some cell components. To take out the cell components guar gum was diluted in milliQ water and afterwards the solution was centrifuged. In this

case the particle size analyzer measured a lot of different peaks. Since the sample was very clear it was hard to measure, due to the low obscuration. Thus, the results were not as reproducible as for the other samples. When guar gum was diluted in milk it was not centrifuged, because otherwise water would have to be added. For comparison also a not centrifuged sample of guar gum in water was measured. The measurement showed a peak at a particle size of 234.1 μm that could be seen in the upper and lower phase of guar gum in milk as well and can be explained by the cell components. For upper as well as lower phase a small peak could be seen at 102 nm and 112 nm, respectively, which was in between the first and second peak of pure milk. For the lower phase additionally one peak at 311 nm could be seen that fits with the third peak of pure milk. In conclusion, it has to be admitted that the measured peaks of the different guar gum samples did not really fit.

Particle size measurements were also performed for iota-carrageenan in milk. The results are shown in figure 23. Dissolving iota-carrageenan in milliQ water produced very clear solutions. Since a certain obscuration is needed to measure particle sizes using static light scattering and this obscuration could not be reached the particle size measurements of iota-carrageenan in water were not reproducible and thus are not shown here. Figure 23 represents the measurement of iota-carrageenan in milk as well as the results of pure milk for comparison. For iota-carrageenan in milk one broad peak was measured that did not fit with any of the milk peaks. It was located at much larger particle sizes namely between 1.1 μm and 282.1 μm. There were little bumps inside this broad peak at 10.8 μm, 25.0 μm and 92.1μm. The particle size was much larger than the size of the milk components as well as what would be expected for a flexible molecule like iota-carrageenan. The particle size and also the broadness of the peak suggest a formation of complexes. Since the casein micelles as well as the iota-carrageenan molecules are negatively charged, a complexation of the negatively charged casein micelles with iota-carrageenan molecules seems unlikely. Another option would be the formation of complexes between iota-carrageenan molecules and whey proteins. As known from the amino acid primary structure and models [45], whey proteins have positive as well as negative surface charges, which suggests the formation of complexes consisting of whey proteins and iota-carrageenan chains. It is worthwhile to mention that the peaks of the pure milk did not show up at all in the iota-carrageenan in milk measurement. This was surprising because it suggests that all milk components participate in the formation of complexes which is unlikely.

The results for the particle size measurements of gellan gum in milk are shown in figure 24. The measurement of gellan gum in water showed one peak at 657 nm and one broad peak between 2.7 μm and 309.6 μm with bumps at 5.1 μm, 22.7 μm, 36.2 μm and 83.9 μm. Gellan gum in milk showed two smaller peaks at 112 nm and 342 nm that to some extent fitted with the second and third peak of pure milk. There was another peak at higher particle sizes (main peak at 176.9 μm) which was shifted compared to gellan gum in water. This behaviour suggests that complexes between whey proteins and gellan gum molecules where formed since gellan gum is negatively charged.

4. Discussion

Concerning milk containing xanthan gum, milk components were detected in the upper (whey proteins) and lower phase (whey proteins and casein micelles). Xanthan gum was solely found in the upper phase which was evidenced by light microscopy of dried droplets, AFM and zeta potential measurements. Moreover, light microscopy, AFM, zeta potential and particle size measurement showed that casein micelles respectively milk components are in the lower phase. From the AFM picture and the remaining turbidity in the upper phase it can be concluded that whey proteins are in the upper phase. The particle size measurement confirms that whey proteins are found in the lower phase as well and none of the other measurements speaks against it.

Xanthan gum is a very stiff and negatively charged molecule. Because of the stiffness it is imagined as a rod in a very simple model. The negatively charged rods repel each other. Also the negatively charged casein micelles repel each other. Furthermore, xanthan gum and casein micelles repel each other. If there were only negatively charged xanthan rods in the volume the charge repulsion would cause a random orientation of the rods. If negatively charged spheres are added to the system one could argue that they are incompatible with the rods. A phase separation where rods are arranged parallel is only possible for non-charged or only slightly charged rods. In the non-charged case a parallel arrangement of the rods would increase the entropy of the system because then the spheres (casein micelles) would have much more states available. But since the xanthan gum rods are strongly negatively charged the electrostatic repulsion is much stronger than the entropic effect. The strong repulsion between the xanthan gum rods causes a demand for maximum distance from each other. A parallel arrangement is very unlikely since all charges along the negatively charged rod repel each other. As a consequence, the strongly negatively charged rods have a random orientation throughout the space available to them. Negatively charged spheres in between the rods would be repelled by the rods but also hinder the arrangement of the rods. The rods had less degrees of freedom to arrange and thus there would not only be an expense of energy but also a decrease in entropy.

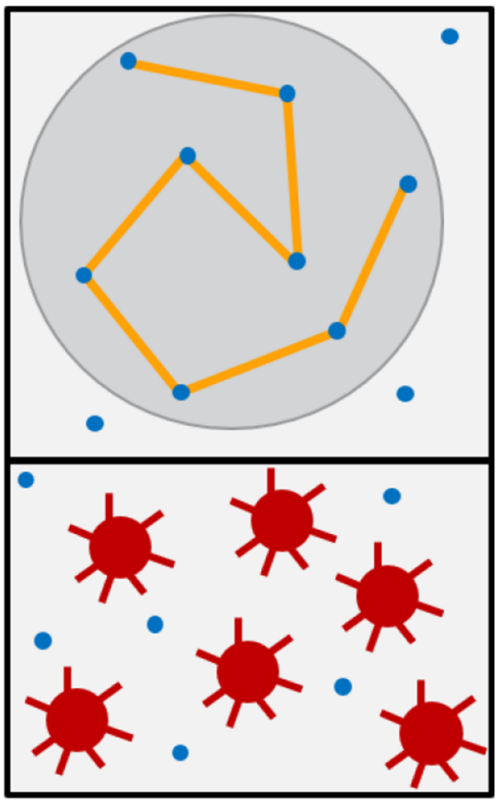

Figure 25. Model for xanthan gum in milk. Multiple xanthan gum rods connect via whey proteins and therefore the excluded volume increases tremendously. Sketch not drawn to scale.

If a whey protein binds to a xanthan gum rod not at its end but somewhere along the rod one could imagine the rod to bend at this position since the charge will be changed at this position. The stiffness of the xanthan gum rod is caused by its highly negatively charged side chains. If a positively charged part of a whey protein binds to one of those negatively charged side chains the potential at this spot is changed. Other parts of the whey protein which are charged negatively will be repelled by the xanthan gum rod. A kinked xanthan gum rod will have a larger excluded volume due to more internal degrees of freedom than a straight one. Thus, the space available to other (kinked) rods and casein micelles would be reduced. If these excluded volumes are larger than the volume of a casein micelle phase separation due to depletion interaction would be conceivable.

Whey proteins can also bind to the end of a xanthan gum rod enabling it to link to another xanthan gum molecule via the whey protein. If multiple xanthan gum rods would interact via whey proteins and thus form a very long kinked chain an entropic explanation could be considered. This new complex would have a much larger excluded volume (large grey sphere in the sketch) than single xanthan gum rods or whey proteins. Then a depletion interaction would cause the phase separation with the larger (larger excluded volume) but lighter (has less weight because it is not really a larger particle) xanthan gum-whey protein-complexes in the upper phase and the smaller but heavier casein micelles in the lower phase. Conceivable examples for configurations of a xanthan gum molecule with a whey protein are shown in the appendix.

A model illustrating the explained behaviour of xanthan gum in milk is shown in figure 25.

The casein micelles and some of the whey proteins are always in the lower phase. The casein micelles are drawn as red spheres with little arms symbolizing the hydrophilic and negatively charged part of the κ-casein. Whey proteins are drawn in a very simple model as blue dots. The xanthan gum molecules are to be found in the upper phase. They are drawn as orange rods. Such a model seems to be most probable, since the xanthan gum molecules are least repelled by whey proteins and keep large degrees of freedom. The model has to be considered a dynamic one. Linkages between xanthan gum molecules via whey proteins are no strong bonds but can be imagined to be broken and formed again with another molecule.

In the light of the current data it is not possible to understand the interactions between the different whey proteins and hydrocolloids in full detail. Each of the different whey proteins features a complex structure, which is slightly different for each of the whey proteins. However, their surface is similarly amphiphilic. Thus, from a theoretical viewpoint the difference should not be too specific. A preciser investigation of the interaction of differently structured whey proteins (see figure 2) with the hydrocolloids requires adaptive

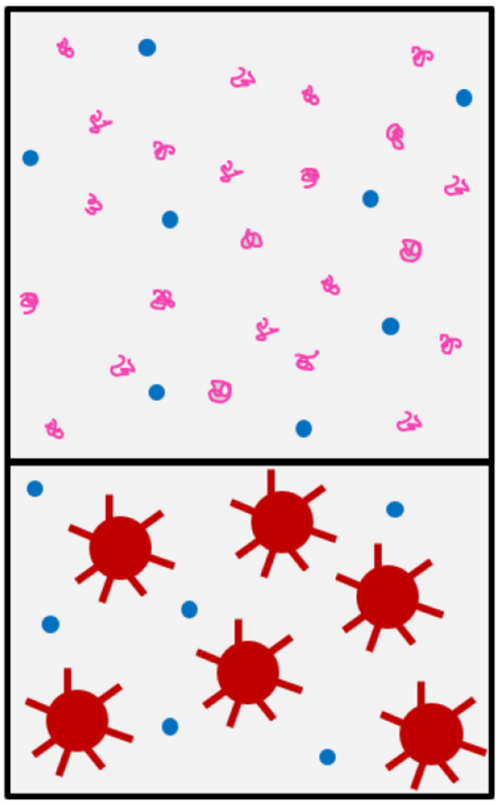

Figure 26. Model for guar gum in milk. The phase separation can be explained by depletion interaction. Sketch not drawn to scale.

computer simulation techniques [46], which are beyond the scope of the present work. A future study on atomistic or adaptive simulations could give more insight. It will be interesting to pursue the present type of study also there with the aim of further consolidating the classification of different interaction mechanisms and their balance.

For guar gum the picture seems to be easier to explain. It was discovered that the guar gum molecules are most likely in the upper phase whereas the casein micelles are in the lower phase. Probably whey proteins are to be found in both phases. Guar gum is uncharged and thus a very flexible molecule being capable of forming random walk coils. These guar gum coils are much smaller than the casein micelles. The phase separation in milk can then be explained by depletion interaction, which is an entropic effect. It is entropically favourable that the larger casein micelle spheres cluster together, because then more states are available to the smaller guar gum coils. This assumption is backed by Tuinier *et al* [18]. Figure 26 shows a sketch of this system.

For iota-carrageenan and gellan gum no macroscopic phase separation could be observed. In these cases the particle size measurements indicated that complexes are likely to be formed. It could be imagined that the hydrocolloid forms complexes with the whey proteins. These complexes could maybe have a similar size as the casein micelles and an overall negative net charge. Thus, casein micelles and complexes of whey protein and hydrocolloid would be distributed throughout the sample. So the coulomb interaction would stabilize the system. Since especially the iota-carrageenan molecules but also the gellan gum molecules are much more flexible than the xanthan gum molecules a complexation is more likely than in the xanthan gum case. If iota-carrageenan molecules, respectively, gellan gum molecules form complexes with the whey proteins, they will loose entropy. But in this case the casein micelles will gain entropy since more states will be available to them. It seems that this entropy gain is predominating and such a configuration is favourable for the system. A sketch for this scenario is drawn in figure 27.

5. Conclusions

There are a variety of food-grade hydrocolloids that are used by the food industry to control rheological properties like viscosity enhancement, thickening, or gel formation of food products as well as to ensure the stability of beverages. However, it was observed that some hydrocolloids provoke a phase separation when

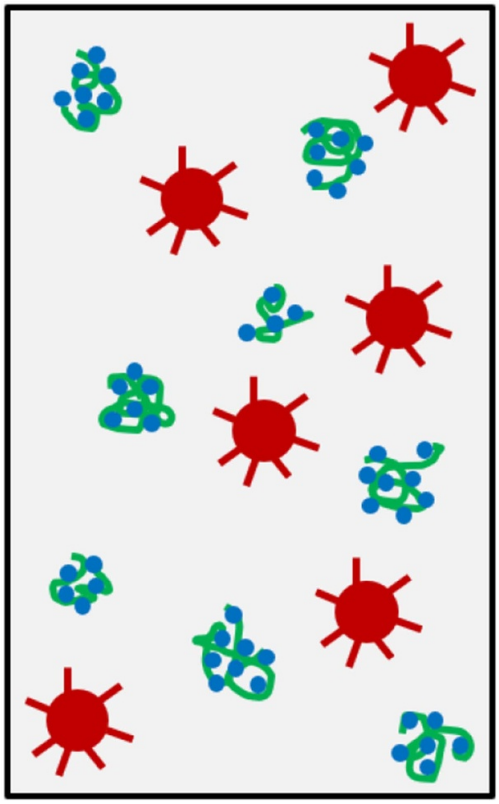

Figure 27. Model explaining the behaviour of iota-carrageenan in milk as well as gellan gum in milk. Sketch not drawn to scale.

added to milk whereas others do not. The goal of this study was to understand the hydrocolloid-milk protein interactions of xanthan gum, guar gum, iota-carrageenan and gellan gum, respectively, that influence the observed macroscopic behaviour. The systems of interest were each of the hydrocolloids dissolved in pasteurized, non-homogenized, skimmed milk (skimmed *Heumilch*). For this industrially motivated research project a hydrocolloid concentration of 0.1 wt% was chosen for all four systems to keep the concentrations below the overlap concentration and to keep the viscosity sufficiently low. At these concentrations, the hydrocolloid in milk mixture remains liquid which is a key property for stabilising milk-based beverages to keep the ''drinkablilty'' in the usual consumers range. Higher concentrations increase significantly the viscosity and require discussions of the contributions of entanglements diffusion and viscosities, which change their scaling laws significantly (see e.g. de Gennes [5] or Doi, Edwards [47]). To investigate these systems optical microscopy, measurement of zeta potentials, atomic force microscopy (AFM) as well as measurement of particle sizes were used.

The chosen hydrocolloids have different physical and chemical properties, like flexibility of the molecule, charge, molecular weight and functional groups. These properties influence the molecule's behaviour in milk and its interaction with the milk proteins. Xanthan gum consists of very stiff molecules with highly negatively charged side chains. The stiffness of the molecule could be observed in AFM images. The zeta potential measurement showed that xanthan gum is the most negatively charged molecule among the four investigated hydrocolloids. When mixed with milk xanthan gum provokes a phase separation. Guar gum in contrast consists of very flexible and uncharged molecules which contain a short uncharged side chain per repeating unit. The AFM images of guar gum dissolved in milliQ water confirmed the assumption that guar gum is forming random walk coils. Even though the molecule shows very different physical and chemical properties compared to xanthan gum, guar gum also provokes a phase separation when added to milk. Iota-carrageenan is quite flexible but negatively charged. The molecule does not contain any side chains. For the case of iota-carrageenan dissolved in milk no macroscopic phase separation could be observed. Gellan gum is also a negatively charged molecule. According to the zeta potential measurement it is stronger negatively charged than iota-carrageenan but less negatively charged than xanthan gum. The negative charge is located at the backbone. The molecule also contains two short uncharged side chains per repeating unit. It is more flexible than the xanthan gum molecule, but less flexible than the iota-carrageenan molecule due to its stronger negative charge compared to iota-carrageenan and the steric hindrance caused by the short uncharged side chains. When gellan gum was added to milk no macroscopic phase separation could be observed.

For the case of xanthan gum dissolved in milk light microscopy of dried droplets and AFM clearly showed that xanthan gum molecules are in the upper phase, which was also suggested by zeta potential measurements. Macroscopic observation and AFM images suggest that also some of the whey proteins are in the upper phase. The AFM images indicate that xanthan gum is interacting with whey proteins and forming a network. Light microscopy of dried droplets, measurement of zeta potential and measurement of particle sizes indicate that milk constituents are found in the lower phase. These measurements also suggest that almost no xanthan gum molecules are in the lower phase. The AFM images confirm that casein micelles and some of the whey proteins are in the lower phase. The phase separation in milk is caused by the stiffness and strong negative charge of the xanthan gum molecules.

In the case of guar gum dissolved in skimmed non-homogenized milk the results of light microscopy of dried droplets indicate that almost all guar gum molecules are in the upper phase whereas the milk constituents are in the lower phase. The AFM images show casein micelles in the lower phase and whey proteins in the upper phase. Unfortunately guar gum molecules could not be observed besides milk components in the AFM images. AFM images have shown that almost all casein micelles are present in the lower phase, suggesting depletion of the casein micelles caused by the guar gum molecules.

For iota-carrageenan and gellan gum a similar picture emerged. In both cases no macroscopic phase separation was observed. Images taken by light microscope revealed that hydrocolloid as well as milk components are distributed throughout the whole droplet. The particle sizes measured suggest the formation of complexes. Since the casein micelles as well as iota-carrageenan and gellan gum, respectively, are negatively charged and whey proteins have positive as well as negative surface charges, it is assumed that the negatively charged hydrocolloids form complexes with the whey proteins. The slightly more negatively charged zeta potential value for gellan gum in milk than for pure milk may be another indicator that complexes are formed. In the AFM images iota-carrageenan, respectively, gellan gum was not visible besides the milk constituents in the same picture due to the scale of the images. The observed particles in these pictures are milk components, or might possibly be complexes between hydrocolloids and whey proteins.

Acknowledgments

Many thanks to Jungbunzlauer Ladenburg GmbH, Dr Albert-Reimann-Strasse 18, 68526 Ladenburg, Germany, for funding this study. Especially to Natalie Dietz, Johanna Kurrat and Nadja Radwan for their kind supervision of the project.

Furthermore, we thank the analytics service group of the Max Planck Institute for Polymer Research in Mainz for measuring the molar masses of the hydrocolloids.

Appendix A. Atomic force microscope

A.1. Droplet evaporation of hydrocolloid in water samples

Figure A1 shows AFM pictures of evaporated droplets of the four hydrocolloids xanthan gum, guar gum, iota-carrageenan and gellan gum in comparison.

As already seen in the pictures of argon dried samples displayed in section 3.5 xanthan gum looks most stiff. Gellan gum looks more flexible than xanthan gum. Iota-carrageenan seems to be even more flexible. However, the guar gum coils look surprisingly stiff and are oriented into the same direction. This behaviour might be explained by an interaction of the very flexible guar gum molecules with the mica surface during slow drying.

A.2. Size determination of particles in AFM images

Sizes of particles in AFM images were measured using the Gwyddion software. In the following (figures A2–A7) screenshots are displayed that show which distances were measured. The corresponding values are listed on the left.

Appendix B. Discussion

In the following (figures B1–B3) examples of configurations that are conceivable for the formation of complexes between multiple xanthan gum rods and whey proteins in figure 25 are shown. The thick red lines symbolise a part of a negatively charged xanthan gum rod. The surface of the whey proteins is shown where positive surface charges are marked blue and negative surface charges red. The representations of the whey proteins were taken from *swissmodel* [12, 45].

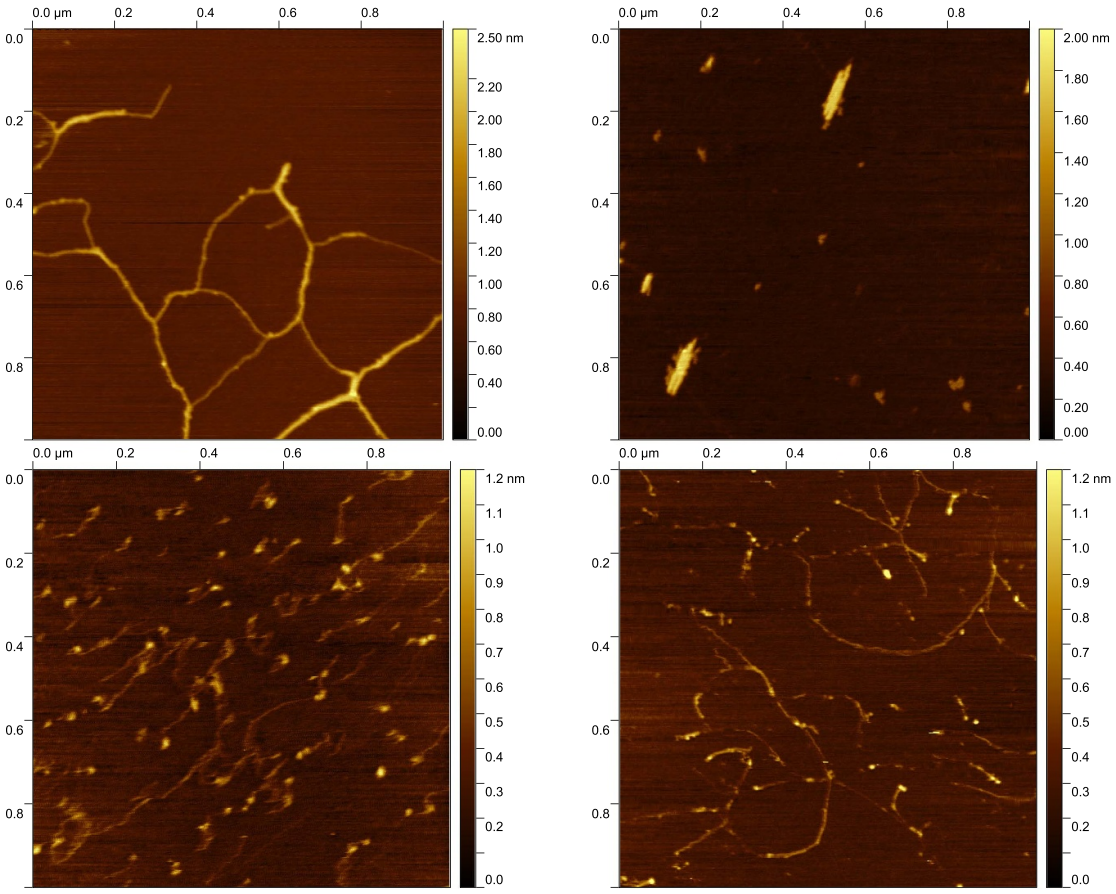

Figure A1. Comparison of the different hydrocolloids. AFM images of evaporated droplets of xanthan gum (upper left), guar gum (upper right), iota-carrageenan (lower left) and gellan gum (lower right) dissolved in milliQ water. The samples had a concentration of 1 μg g^{-1} before drying. The scan size of each image is 1 μm.

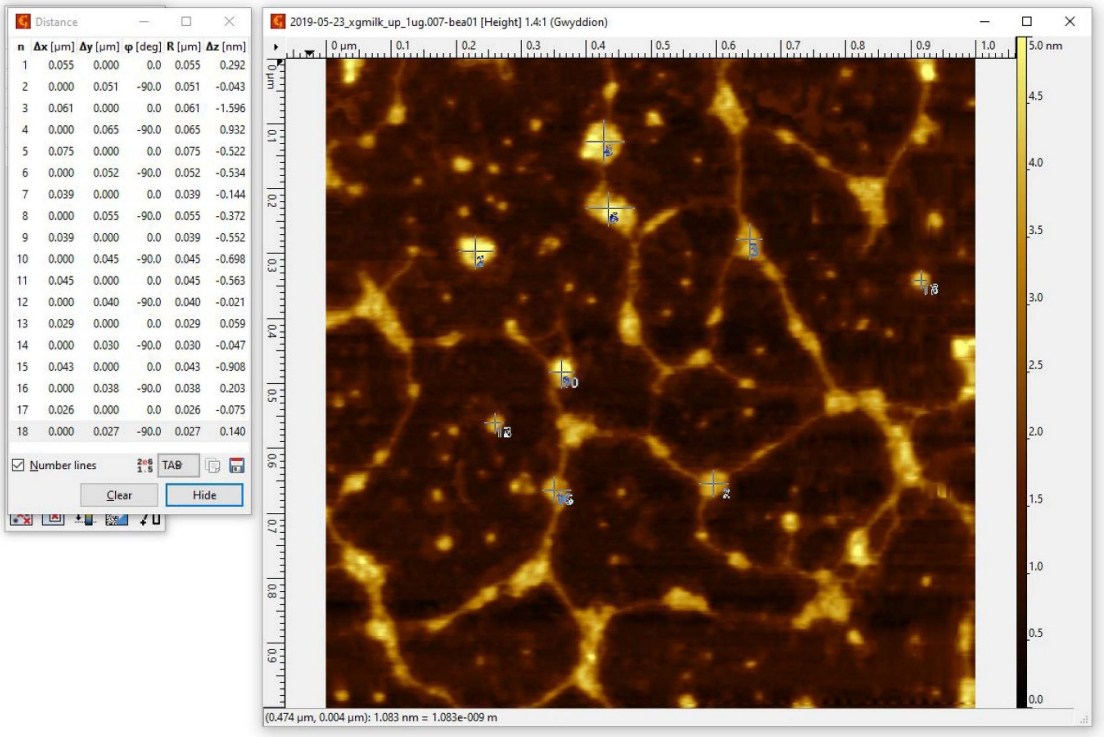

Figure A2. Diameter determination in the upper phase of xanthan gum dissolved in milk.

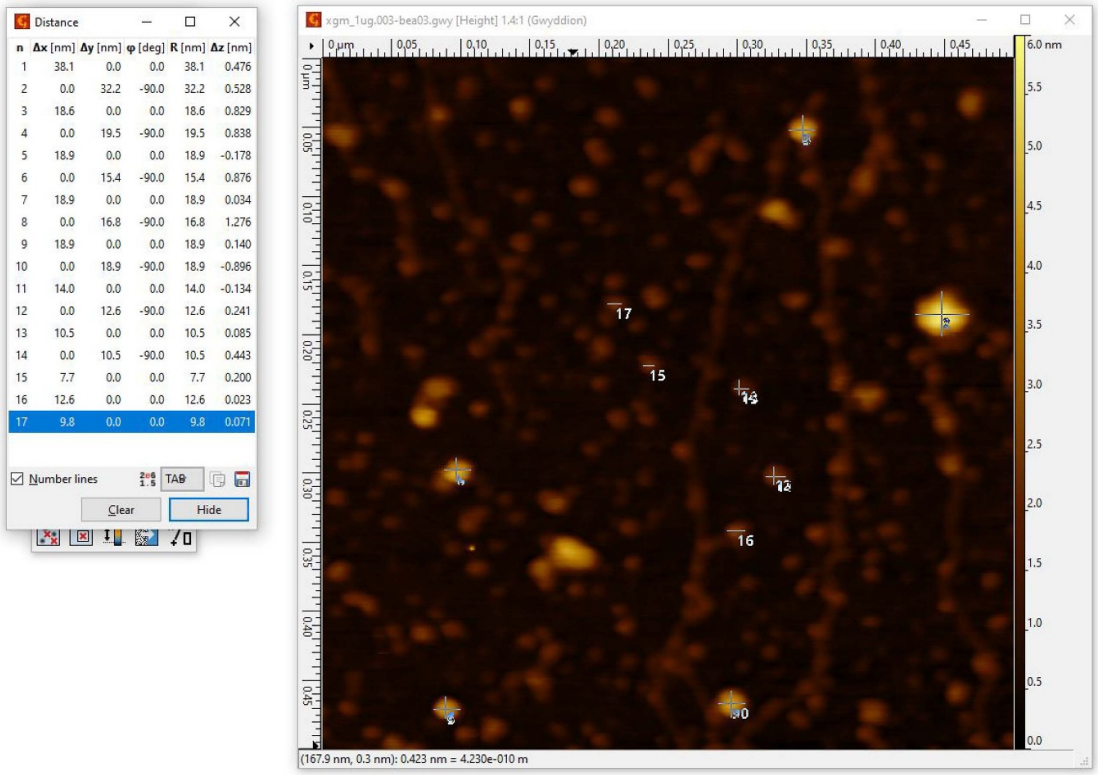

Figure A3. Diameter determination in the upper phase of xanthan gum dissolved in milk.

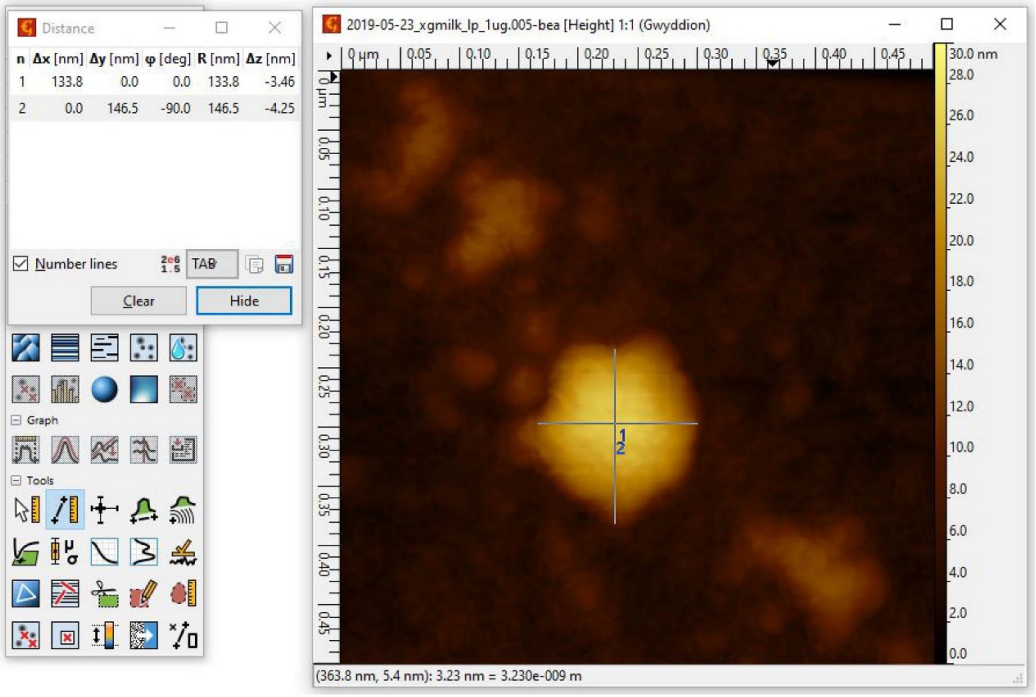

Figure A4. Diameter determination of a casein micelle in the lower phase of xanthan gum dissolved in milk.

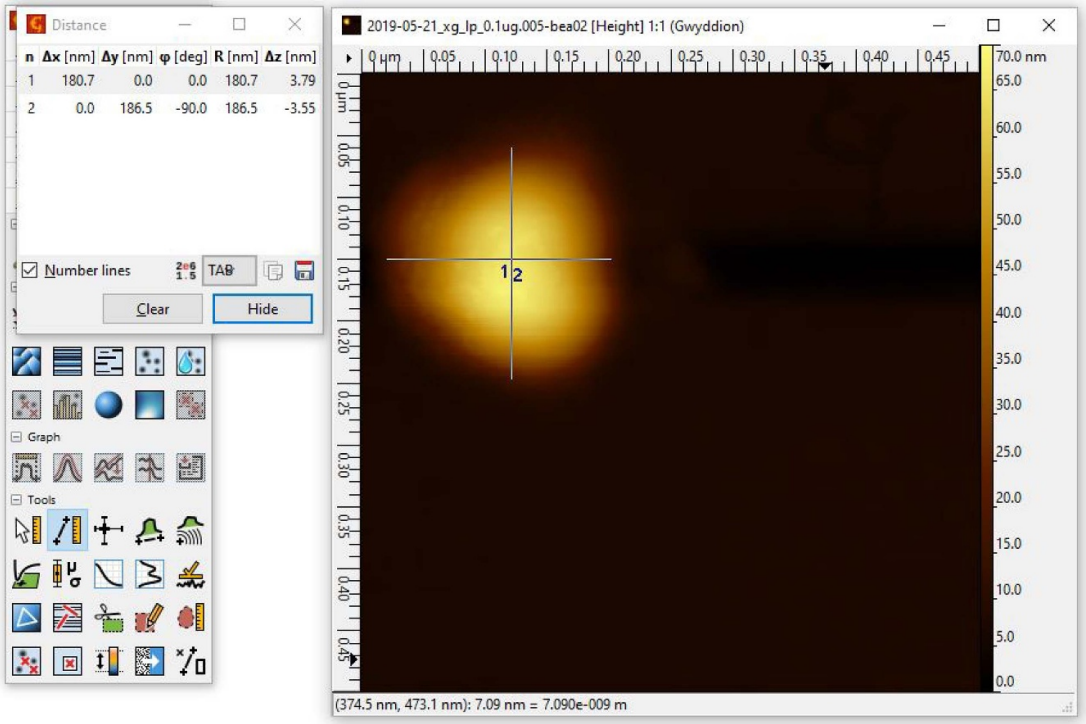

Figure A5. Diameter determination of a casein micelle in the lower phase of xanthan gum dissolved in milk.

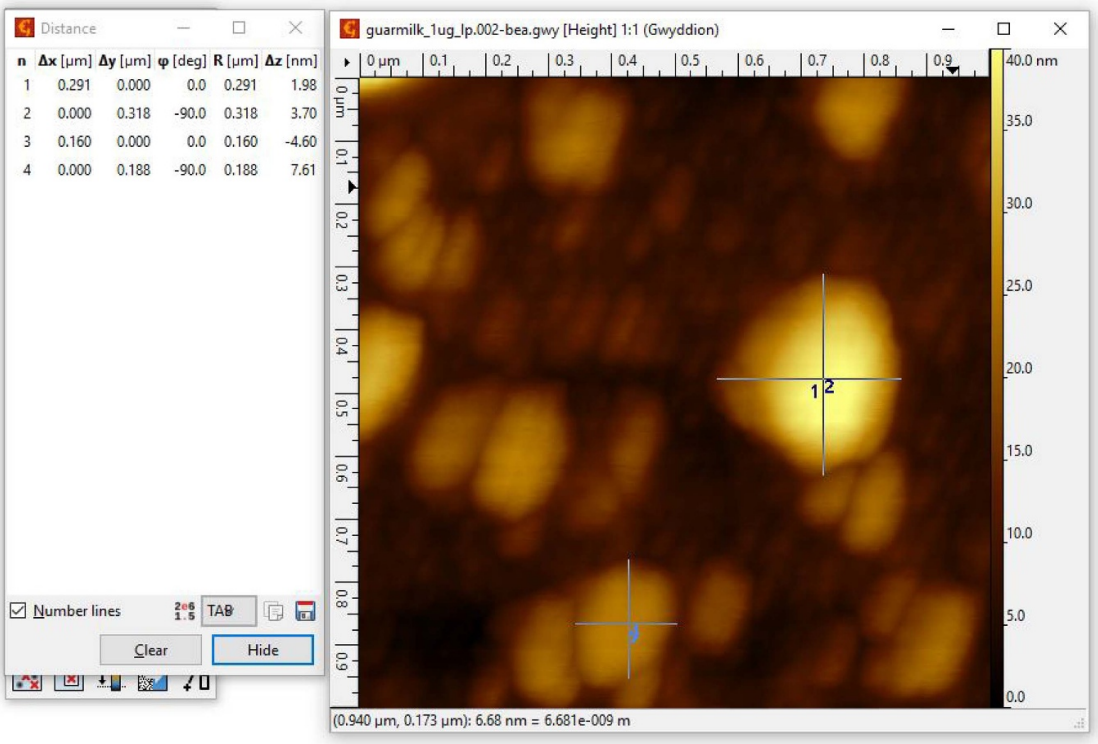

Figure A6. Diameter determination of particles in the upper phase of guar gum dissolved in milk.

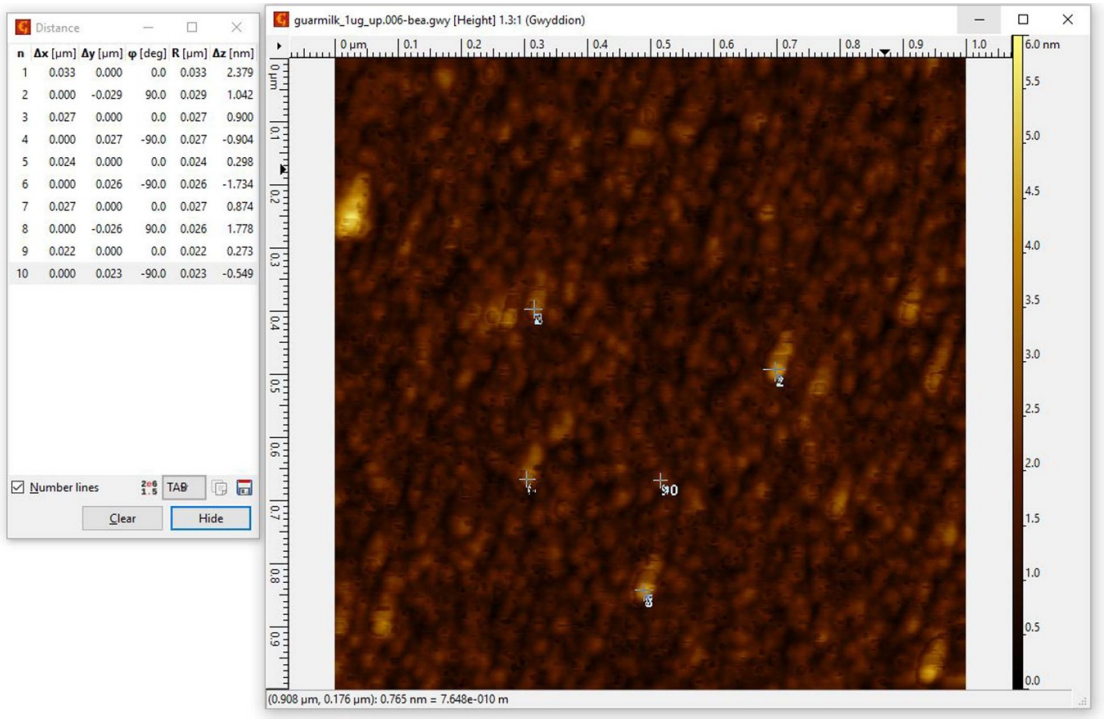

Figure A7. Diameter determination of particles in the lower phase of guar gum dissolved in milk.

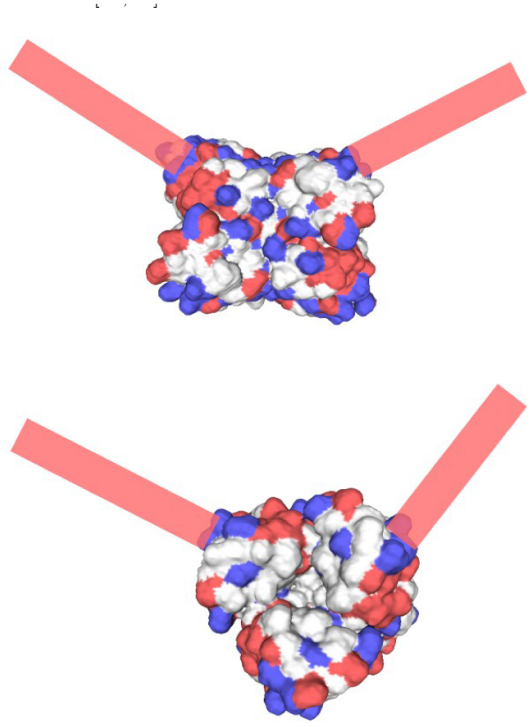

Figure B1. Configurations for the interaction of xanthan gum with α-lactalbumin. Not drawn to scale.

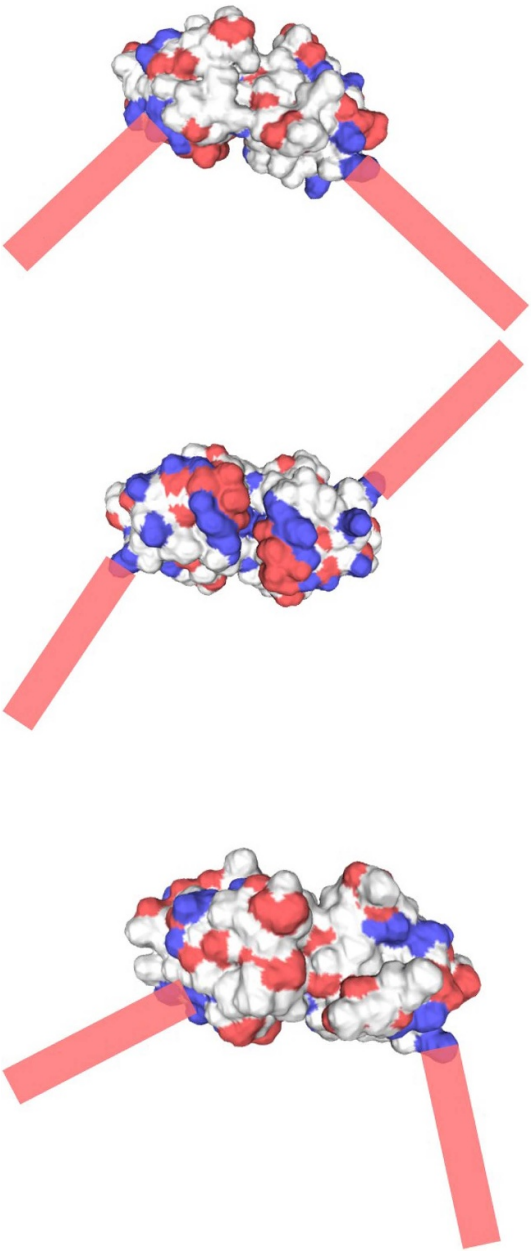

Figure B2. Configurations for the interaction of xanthan gum with β-lactoglobulin. Not drawn to scale.

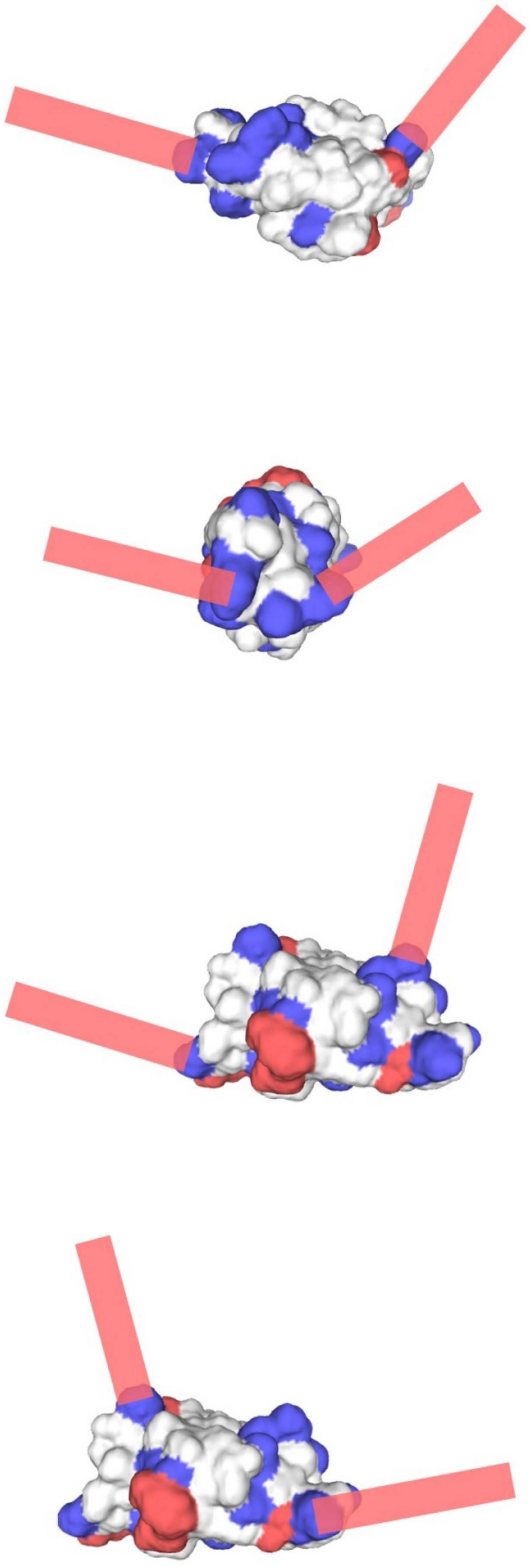

Figure B3. Configurations for the interaction of xanthan gum with serum albumin. Not drawn to scale.

ORCID iDs

Judith Hege https://orcid.org/0000-0003-0016-3320
Thomas Palberg https://orcid.org/0000-0002-3443-8479
Thomas A Vilgis https://orcid.org/0000-0003-2101-7410

References

[1] Belitz H D, Grosch W and Schieberle P 2009 Food chemistry *Milk and Dairy Products* (Berlin: Springer) pp 498–545
[2] Ha E and Zemel M B 2003 Functional properties of whey, whey components, and essential amino acids: mechanisms underlying health benefits for active people (review) *J. Nutritional Biochem.* **14** 251–8
[3] Glicksman M 2020 *Food Hydrocolloids* vol 1 (Boca Raton, FL: CRC Press)
[4] Williams P A and Phillips G O 2009 Introduction to food hydrocolloids *Handbook of Hydrocolloids* (Amsterdam: Elsevier) pp 1–22
[5] de Gennes P-G 1979 *Scaling Concepts in Polymer Physics* (Ithaca and London: Cornell University Press)
[6] Töpel A 2016 Chemie und Physik der Milch 4th edn (Hamburg: Behr's Verlag)
[7] Ternes W 2008 *Naturwissenschaftliche Grundlagen der Lebensmittelzubereitung* (Hamburg: Behr's Verlag)
[8] Vilgis T A 2014 *Frische Milch - kolloidale Struktur, Physik und Verdauung J. Culinaire* **18** 55–69
[9] De Kruif C G, Huppertz T, Urban V S and Petukhov A V 2012 Casein micelles and their internal structure *Adv. Colloid Interface Sci.* **171–2** 36–52
[10] Vilgis T A 2015 Soft matter food physics - the physics of food and cooking *Rep. Prog. Phys.* **78** 124602
[11] https://swissmodel.expasy.org/repository/uniprot/P02754 (Accessed: 16th August 2019)
[12] Bienert S, Waterhouse A, de Beer T A P, Tauriello G, Studer G, Bordoli L and Schwede T 2017 The SWISS-MODEL Repository - new features and functionality *Nucleic Acids Res.* **45** D313–D319
[13] https://swissmodel.expasy.org/repository/uniprot/P00711 (Accessed: 16th August 2019)
[14] https://swissmodel.expasy.org/repository/uniprot/P02769 (Accessed: 16th August 2019)
[15] Perez A A, Carrera Sánchez C, Rodríguez Patino J M, Rubiolo A C and Santiago L G 2010 Milk whey proteins and xanthan gum interactions in solution and at the air–water interface: A rheokinetic study *Colloids and Surfaces B: Biointerfaces* **81** 50–7
[16] Van Gruijthuijsen K, Herle V, Tuinier R, Schurtenberger P and Stradner A 2012 Origin of suppressed demixing in casein/xanthan mixtures *Soft Matter* **8** 1547–55
[17] Bourriot S, Garnier C and Doublier J-L 1999 Phase separation, rheology and structure of micellar casein-galactomannan mixtures *Int. Dairy J.* **9** 353–7
[18] Tuinier R, ten Grotenhuis E and de Kruif C G 2000 The effect of depolymerised guar gum on the stability of skim milk *Food Hydrocolloids* **14** 1–7
[19] Buldo P, Benfeldt C, Carey J P, Folkenberg D M, Jensen H B, Sieuwerts S, Vlachvei K and Ipsen R 2016 Interactions of milk proteins with low and high acyl gellan: Effect on microstructure and textural properties of acidified milk *Food Hydrocolloids* **60** 225–31
[20] Garnier C, Michon C, Durand S, Cuvelier G, Doublier J-L and Launay B 2003 Iota-carrageenan/casein micelles interactions: evidence at different scales *Colloids and Surfaces B: Biointerfaces* **31** 177–84
[21] Langendorff V, Cuvelier G, Michon C, Launay B and Parker A de Kruif C G 2000 Effects of carrageenan type on the behaviour of carrageenan/milk mixtures *Food Hydrocolloids* **14** 273–80
[22] Stephen A M 2006 *Food Polysaccharides and Their Applications* 2nd edn (Boca Raton: Taylor and Francis)
[23] Imeson A 2010 *Food Stabilisers, Thickeners and Gelling Agents* (Oxford: Wiley-Blackwell)
[24] Lekkerkerker H N W and Tuinier R 2011 Depletion interaction *Colloids and the Depletion Interaction* (Berlin: Springer) pp 57–108
[25] Jensen R G 1995 *Handbook of Milk Composition* (New York: Academic)
[26] Schönherr H and Vancso G J 2010 Atomic force microscopy in practice *Scanning Force Microscopy of Polymers* (Berlin: Springer) pp 25–75
[27] Hunter R J 2013 *Zeta Potential in Colloid Science: Principles and Applications* (New York: Academic)
[28] Kuntsche J, Klaus K and Steiniger F 2009 Size Determinations of Colloidal Fat Emulsions: A Comparative Study *J. Biomed. Nanotechnol.* **5** 384–95
[29] Gaucheron F 2005 The minerals of milk *Reprod. Nutr. Dev.* **45** 473–83
[30] O'Connell J E, Fox P D, Tan-Kintia R and Fox P F 1998 Effects of Tea, Coffee and Cocoa Extracts on the Colloidal Stability of Milk and Concentrated Milk *Int. Dairy J.* **8** 689–93
[31] Trejo R, Dokland T, Jurat-Fuentes J and Harte F 2011 Cryo-transmission electron tomography of native casein micelles from bovine milk *J Dairy Sci.* **94** 5770–5
[32] Elliott R P and Michener H D 1965 Factors Affecting The Growth Of Psychrophilic Micro-Organisms In Foods: A Review (Washington, DC: USDA Technical Bulletin No. 1320)
[33] Cousin M A 1982 Presence and Activity of Psychrotrophic Microorganisms in Milk and Dairy Products: A Review *J. Food Pro.* **45** 172–207
[34] Kraft A A and Rey C R 1979 Psychrotrophic bacteria in foods: An update *Food Technol.* **33** 66–71
[35] www.glaeserne-molkerei.de (Accessed: 28th August 2019)
[36] https://www.nzmp.com/content/dam/nzmp/pdfs/nzmp-whey-protein-isolate-infographic.pdf (Accessed: 12th September 2019)
[37] Nečas D and Klapetek P 2019 Gwyddion http://gwyddion.net/ (Accessed: 30th March 2020)
[38] Inc. Beckman Coulter 2009 LS 13 320 Laser Diffraction Particle Size Analyzer Instrument Manual (Brea, CA: Beckman Coulter, Inc.)
[39] https://imagej.nih.gov/ij/ (Accessed: 30th March 2020)
[40] Skender A, Hadj-Ziane-Zafour A and Flahaut E 2013 Chemical functionalization of Xanthan gum for the dispersion of double-walled carbon nanotubes in water *Carbon* **62** 149–56
[41] Rubinstein M and Colby R H 2008 *Polymer Physics* (New York: Oxford University Press Inc.)
[42] Fox P F and McSweeney P L H 2003 *Advanced Dairy Chemistry - 1 Proteins* 3rd edn (New York: Springer)
[43] Surve M, Pryamitsyn V and Ganesan V 2005 Depletion and pair interactions of proteins in polymer solutions *J. Chem. Phys.* **122** 154901
[44] Bürkle G 2016 Viskosität von Flüssigkeiten https://www.buerkle.de/files_pdf/wissenswertes/viskositaeten_de_2016.pdf (Accessed: 25th October 2019)

[45] https://swissmodel.expasy.org/ (Accessed: 18th October 2019)
[46] Fiorentini R, Kremer K, Potestio R and Fogarty A C 2017 Using force-based adaptive resolution simulations to calculate solvation free energies of amino acid sidechain analogues *J. Chem. Phys.* **146** 244113
[47] Doi M and Edwards S F 1988 *The Theory of Polymer Dynamics* (Oxford: Clarendon)